

**SYSTEM-WIDE SUBMERGED AQUATIC VEGETATION  
MODEL FOR CHESAPEAKE BAY**

Carl F. Cerco<sup>1</sup>  
US Army Engineer Research and Development Center  
3909 Halls Ferry Road  
Vicksburg, MS  
601-634-4207 (voice)  
601-634-3129 (fax)  
Cerco@homer.wes.army.mil

Kenneth Moore  
Virginia Institute of Marine Science  
College of William and Mary  
Gloucester Point VA 23062  
804-684-7384 (voice)  
Moore@vims.edu

---

<sup>1</sup>Corresponding author

## Abstract

A predictive model of submerged aquatic vegetation (SAV) biomass is coupled to a eutrophication model of Chesapeake Bay. Domain of the model includes the mainstem of the bay as well as tidal portions of major embayments and tributaries. Three SAV communities are modeled: ZOSTERA, RUPPIA, and FRESHWATER. The model successfully computes the spatial distribution and abundance of SAV for the period 1985-1994. Spatial distribution is primarily determined by computed light attenuation. Sensitivity analysis to reductions in nutrient and solids loads indicates nutrient controls will enhance abundance primarily in areas that presently support SAV. Restoration of SAV to areas in which it does not presently exist requires solids controls, alone or in combination with nutrient controls.

## Introduction

Approximately thirty years ago, submerged aquatic vegetation (SAV) in Chesapeake Bay commenced an unprecedented decline. By the early 1980's, the distribution and abundance of SAV reached a historic low point (Orth and Moore 1984). Consensus centered on increased light attenuation as the mechanism behind the decline (Kemp et al. 1983; Twilley et al. 1985). The increased attenuation was attributed directly to increased concentrations of fixed solids and, indirectly, to increased concentrations of nutrients in the water column. The nutrients stimulate the growth of planktonic and epiphytic algae, thereby diminishing light available to SAV leaves. Following the decline, restoration of the SAV community, largely through controls on nutrient loads, has been a cornerstone of bay management policy (Baliles et al. 1987).

Initial efforts to evaluate the benefit of nutrient controls on SAV relied on living-resources habitat criteria. A system-wide eutrophication model (Cerco and Cole 1993) was used to estimate chlorophyll concentration, nutrient concentrations, and light attenuation. These were compared to living-resources criteria (Dennison et al. 1993) and potential benefits to SAV were implied. The living-resources criteria approach had two shortcomings. First, only qualitative, not quantitative improvements were implied. Second, feedback effects between improved SAV abundance and the surrounding environment were omitted. For example, the damping effect of SAV on suspended solids (Ward et al. 1984) could not be computed. As a consequence of these shortcomings, the decision was made to incorporate an SAV sub-model into the eutrophication model. This SAV sub-model directly simulates SAV abundance, distribution, and interactions between SAV and the environment.

Three components are required to make up a system-wide SAV model. The first is a unit-level model of a plant. The second is an environmental model that provides light, temperature, nutrient concentrations, and other forcing functions to the plant component. The third is a coupling algorithm that links the system-wide environmental model to the local-scale plant model. The environmental model has been largely previously described (Cerco and Cole 1993). Significant improvements to the model since original publication include a refined, finer-scale grid and simulation of suspended solids concentrations (Cerco and Meyers 2000). In this paper, we describe the unit model, the coupling between the unit model and the environmental model, and results of the application of the system-wide SAV model.

## Methods

### The Submerged Aquatic Vegetation Unit Model

The SAV unit model (Fig. 1) incorporates three state variables: shoots (above-ground biomass), roots (below-ground biomass), and epiphytes (attached growth). Epiphytes and shoots exchange nutrients with the

water-column component of the eutrophication model while roots exchange nutrients with the diagenetic sediment component (DiToro and Fitzpatrick 1993). Light available to the shoots and epiphytes is computed via a series of sequential attenuations by color, fixed and organic solids in the water column, and by self-shading of shoots and epiphytes. The selection of state variables and basic principles of the model were based on principles established by Wetzel and Neckles (1986) and Madden and Kemp (1996).

### Shoots

The governing equation for shoots establishes a balance between sources and sinks of above-ground biomass:

$$\frac{d \text{ SH}}{dt} = (\text{P} \bullet (1 - \text{Fpsr}) - \text{Rsh} - \text{SL}) \bullet \text{SH} + \text{Trs} \bullet \text{RT}$$

in which SH = shoot biomass ( $\text{g C m}^{-2}$ ); P = production ( $\text{d}^{-1}$ ); Fpsr = fraction of production routed from shoot to root; Rsh = shoot respiration ( $\text{d}^{-1}$ ); SL = sloughing ( $\text{d}^{-1}$ ); Trs = rate at which carbon is transported from root to shoot ( $\text{d}^{-1}$ ); and RT = root biomass ( $\text{g C m}^{-2}$ ).

Production is computed as the product of a specified maximum rate (a function of temperature) and a limiting factor. The limiting factor is the minimum of independently evaluated light, nitrogen, and phosphorus limitations. Light limitation is selected from one of several functions (Jassby and Platt 1976) that fit observed production versus irradiance curves:

$$f(I) = \frac{I_{sh}}{\sqrt{I_{sh}^2 + I_k^2}}$$

in which  $f(I)$  = light limitation; and  $I_{sh}$  = irradiance at leaf surface ( $\text{E m}^{-2} \text{ day}^{-1}$ ). Parameter  $I_k$  is derived from two specified parameters:

$$I_k = \frac{P_{\max}(T)}{\alpha}$$

in which  $P_{\max}$  = maximum production as a function of temperature ( $\text{g C g}^{-1} \text{ DW d}^{-1}$ ) and  $\alpha$  = initial slope of production versus irradiance curve ( $\text{g C g}^{-1} \text{ DW} (\text{E m}^{-2})^{-1}$ ).

Nutrient limitations for nitrogen and phosphorus are evaluated using a formula (Madden and Kemp 1996)

$$f(N) = \frac{N_w + K^* \bullet N_s}{K_{hw} + N_w + K^* \bullet N_s}$$

that combines individual Monod-like functions for the roots and shoots:

in which  $f(N)$  = nutrient limitation;  $N_w$  = nutrient concentration ( $\text{g m}^{-3}$ ) in water column,  $N_s$  = nutrient concentration ( $\text{g m}^{-3}$ ) in sediment pore water;  $K_{hw}$  = half-saturation concentration for nutrient uptake by shoots ( $\text{g m}^{-3}$ );  $K_{hs}$  = half-saturation concentration for nutrient uptake by roots ( $\text{g m}^{-3}$ ); and  $K^* = K_{hw} / K_{hs}$ .

## Roots

The governing equation for roots establishes a balance between sources and sinks of below-ground biomass:

$$\frac{d RT}{dt} = F_{psr} \bullet P \bullet SH - R_{rt} \bullet RT - Trs \bullet RT$$

in which  $R_{rt}$  = root respiration ( $d^{-1}$ ).

## Epiphytes

$$\frac{d EP \bullet SH}{dt} = (Pep \bullet DL - Rep - PR \bullet EP - SL) \bullet SH \bullet EP$$

Epiphytes are quantified as mass per unit of shoot mass:

in which EP = epiphyte abundance (g epiphyte C  $g^{-1}$  shoot carbon); Pep = epiphyte production ( $d^{-1}$ ); DL = density limitation function; Rep = epiphyte respiration ( $d^{-1}$ ); and PR = predation on epiphytes (g shoot C  $g^{-1}$  epiphyte carbon  $d^{-1}$ ). The formulation provides a change in epiphyte abundance as a function of epiphyte processes and shoot processes. Net production of epiphytes without corresponding production of shoots results in an increase in epiphyte abundance on the shoots. Net production of shoots without corresponding epiphyte production results in diminished epiphyte abundance. Sloughing results in loss of attached epiphytes and produces no net change in abundance. The density limitation function diminishes production as leaf substrate becomes filled with epiphytes.

Epiphyte production is modeled as a function of light, nutrients, and temperature. Light effects are computed using formulae similar to Equations 2 and 3 while nutrient effects are evaluated with conventional Monod functions. Neckles et al. (1993) showed that predation can be an important limitation on epiphyte abundance.

Absence of data prevents inclusion of predators in the model, however. Instead, a linear proportionality between predators and prey is assumed. Parameter PR incorporates both the proportionality and predation rate and is evaluated empirically.

## SAV Composition and Nutrient Cycling

A fundamental assumption of the model is that plants have uniform, constant composition. Nitrogen and phosphorus in plant biomass are quantified as fractions of the carbonaceous biomass. Nutrients are taken up in stoichiometric relation to net production. Proportions removed from the water column and sediments are determined by the relative nutrient limits in each pool. Respiration and sloughing return appropriate quantities of nutrients to the sediments and water column.

## The Light Field

A conceptual model has been long-established in which light reaching SAV shoots is first attenuated by dissolved and particulate matter in the water column and next by epiphytic material (e.g. Kemp et al. 1983). The representation of self-shading by shoots and by epiphytes and potential shading of epiphytes by SAV is murkier. One approach is to incorporate density-limiting functions into the model that simulate both self-shading and space limitations (Wetzel and Neckles 1986; Madden and Kemp 1996). The density-limit

approach is adopted here for epiphytes since it appears reasonable that epiphyte abundance will ultimately be limited by leaf substrate available for attachment. The concept of a space limitation on SAV shoots is less appealing, however. Consequently, self shading by SAV shoots is considered explicitly.

Light available to SAV shoots is computed through a series of sequential attenuations. First, light at the top

$$I_c = I_o \cdot e^{-(K_w + K_i \cdot ISS + K_v \cdot VSS) \cdot Z_{tc}}$$

of the canopy is computed:

in which  $I_c$  = light at the canopy top ( $E\ m^{-2}\ day^{-1}$ );  $I_o$  = light at water surface ( $E\ m^{-2}\ day^{-1}$ );  $K_w$  = attenuation due to color ( $m^{-1}$ );  $K_i$  = attenuation coefficient for fixed solids ( $m^2\ g^{-1}$ );  $ISS$  = fixed solids concentration ( $g\ m^{-3}$ );  $K_v$  = attenuation coefficient for volatile solids ( $m^2\ g^{-1}$ );  $VSS$  = volatile solids concentration ( $g\ m^{-3}$ ); and  $Z_{tc}$  = depth to canopy (m).

Next, mean light within the canopy is evaluated. Assuming that attenuation by shoots follows an exponential

$$I_{wc} = \frac{I_c}{K_{sh} \cdot SH} \cdot (1 - e^{-K_{sh} \cdot SH})$$

relationship analogous to Equation 7 (Titus and Adams 1979), the mean light field within the canopy is: in which  $I_{wc}$  = mean light within the canopy ( $E\ m^{-2}\ day^{-1}$ ); and  $K_{sh}$  = attenuation by SAV shoots ( $m^2\ g^{-1}\ C$ ).  $I_{wc}$  is the light available to epiphytes.

Although epiphyte accumulation in Chesapeake Bay and elsewhere can be related to nutrient concentrations (Kemp et al. 1983; Twilley et al. 1985; Borum 1985), not all epiphytic material is viable algae. Total accumulation of epiphytic material is an order of magnitude greater than viable algae (Fig. 2). A rough proportionality between total accumulation and biomass is maintained over several orders of magnitude of biomass. The proportionality is represented in the model by the quantity  $Adwcep$ , the ratio of total epiphyte dry weight to viable epiphyte carbon. Employing this parameter, light reaching the shoots through the

$$I_{sh} = I_{wc} \cdot e^{-K_{ep} \cdot A_{cla} \cdot Adwcep \cdot EP}$$

epiphyte layer is computed:

in which  $I_{sh}$  = light available to shoots ( $E\ m^{-2}\ day^{-1}$ );  $K_{ep}$  = attenuation by epiphytes ( $m^2\ leaf\ surface\ g^{-1}\ DW$ ); and  $A_{cla}$  = g shoot  $C\ m^{-2}$  leaf area.

#### SAV Effect on Suspended Solids

The damping of wind-generated waves in SAV beds (Ward et al. 1984) results in diminished suspended sediment concentrations relative to concentrations outside the bed (Fig. 3). The effect of SAV on suspended solids is represented by addition of an SAV-dependent net-settling velocity to the mass balance equation for

$$\frac{d\ ISS}{d\ t} = \text{net transport} - \frac{1}{H} \cdot (W_{iss} + W_{sav} \cdot SH) \cdot ISS$$

suspended solids:

in which  $W_{iss}$  = net settling velocity of suspended solids in open water ( $m\ d^{-1}$ );  $W_{sav}$  = enhanced net settling due to SAV ( $m^3\ g^{-1}\ C\ d^{-1}$ ); and  $H$  = local depth (m). Parameter  $W_{iss}$  varies spatially and temporally but has a characteristic value  $0.05\ m\ d^{-1}$ . Value of  $W_{sav}$ ,  $0.05\ m^3\ g^{-1}\ C\ d^{-1}$ , is assigned to reproduce in the model the observed trend.

### From the Unit to the System

The Chesapeake Bay Environmental Model Package (CBEMP) operates by dividing the continuum of the bay into a grid of discrete cells. In the present grid, the surface plane of the bay and its major tributaries is sectioned into 2100 cells with a length scale of 2 km. Width of each cell varies depending on the local geometry. For the SAV model, a ribbon of littoral cells was created along the land-water margin of the system. Width of each littoral cell corresponded to the distance from the two-meter depth contour to the shore. The two-meter depth was selected since restoration of SAV to the two-meter contour is a major goal of the bay management effort (Batiuk et al. 1992). SAV was modeled in these littoral cells and in a few additional cells in regions that historically supported SAV. Littoral cells were represented as having a mean depth of one meter. Depth of the additional cells was determined by local bathymetry and was usually 2 m.

The major problem in coupling the system-wide model with the unit model is the difference in scales represented by the two models. The minimum scale represented by the CBEMP is on the order of km while the scale on which SAV is distributed is orders of magnitude smaller. Three scaling factors were employed to relate biomass on the unit level to abundance on the grid scale. These were: truncation error, coverage, and patchiness (Fig. 4). Truncation error is the ratio of actual area within the two-meter contour to the area of the quadrilateral model cell. Coverage is the fraction of a cell occupied by SAV beds, and patchiness represents

$$M = SH \cdot A \cdot TE \cdot C \cdot P$$

the fraction of bottom area covered by plants within an SAV bed. Abundance within each cell is then:

in which  $M$  = above-ground abundance ( $g\ C$ );  $A$  = cell surface area ( $m^2$ );  $TE$  = truncation error;  $C$  = coverage; and  $P$  = patchiness. Truncation error was determined by comparison of model surface area with actual area determined by a GIS system. The error ranged from 0.2 to 1.55 with a mean value of 0.75. Coverage was assumed to be fifty percent. Patchiness was determined by comparison of computed and observed abundance and was determined to be 0.3 for the FRESHWATER and ZOSTERA communities and 0.8 for the RUPPIA community.

The relationship of shoot (and root) biomass to abundance allowed uptake and release of materials by plants on a unit area basis to be converted to a mass basis for employment in the mass-balance equation applied to each cell (Cercio and Cole 1993).

### The Data Bases

Primary data base for comparison of computed and observed SAV was a monthly time series of above-ground abundance estimates (Moore et al. 2000) for the period 1985-1996. Estimates were provided for four mutually-exclusive SAV community types and were available on an aggregate basis and for each of 44 Chesapeake Bay Program Segments (CBPS). Program segments are subdivisions of the bay determined by mean salinity, natural boundaries, and other features. Thirty-five segments (Fig. 5), having a median area of  $150\ km^2$ , are included in the model grid.

Suspended solids and light attenuation observations were drawn from monitoring data provided by the Chesapeake Bay Program Office (CBPO), Annapolis MD. The CBPO conducts a program in which observations are collected at over 100 stations in 20 surveys per year. For comparison with the model, observations were averaged by month and over CBPS. Light attenuation measures were largely in the form

$$KE = \frac{1.33}{DV}$$

of disk visibility and were converted to attenuation through the relationship: in which KE = diffuse light attenuation ( $m^{-1}$ ); and DV is disk visibility (m). The factor 1.33 was validated through comparison with measures of light penetration conducted in the upper bay (Lacouture, R. Smithsonian Environmental Research Center, Edgewater MD) and is typical for turbid estuarine waters (Holmes 1970; Keefe et al. 1976).

#### Modeled Communities

Three major, mutually-exclusive SAV community types were modeled: ZOSTERA, RUPPIA, and FRESHWATER. Moore et al. (2000) identified a fourth type, POTAMOGETON, but the abundance in this type was negligible compared to the others. Since the distributions of POTAMOGETON and RUPPIA often overlap, the POTAMOGETON community was combined into the RUPPIA community for model purposes. Model cells were assigned a community type (Fig. 6) based on observed distribution and environmental factors (Moore et al. 2000).

#### Parameter Evaluation

##### The SAV Component

Parameter evaluation for the SAV component of the model is both an art and a chore. Although substantial observations exist, especially for the ZOSTERA community, variations in methodology and reporting preclude determination of a definitive set of model parameters. The evaluation procedure consisted of selection of an initial parameter set from the literature, followed by revisions to improve agreement between modeled and observed biomass in CBPS that support substantial SAV communities.

For ZOSTERA, primary data sources included Wetzel and Penhale (1983), Evans et al. (1986), and Marsh et al. (1986). Parameters (Table 1) were selected to optimize agreement between computed and observed shoot and root biomass (Fig. 7). For RUPPIA, primary data sources were Wetzel and Penhale (1983) and Evans et al. (1986). Final parameters (Table 1) were selected to optimize agreement between computed and observed shoot (Fig. 8) and root biomass. Insufficient data were found to assemble monthly means and ranges of root biomass. Observations collected by Moore et al. (1994) over a year indicate a range in root biomass of 0.8 to 13 g C  $m^{-2}$  with a mean of 6.1 g C  $m^{-2}$ . These compare to a model range of 1.7 to 11.3 g C  $m^{-2}$  and mean of 6.1 g C  $m^{-2}$  in segment EE1. For the FRESHWATER community, primary data sources included Van et al. (1976), Bowes et al (1977; 1979), and Barko and Smart (1981). Final parameters (Table 1) were selected to optimize agreement between computed and observed shoot (Fig. 9) and root biomass. As with RUPPIA, insufficient data were found to assemble meaningful monthly means and ranges of root biomass. Available information indicates the roots of freshwater SAV comprise from 4% to 41% of total plant biomass (Haller and Sutton 1975, Barko and Smart 1981). In the model, roots comprised 23% of total plant biomass during the growing season (April - October) in segment CB1.

## Epiphytes

Epiphyte accumulation on natural and artificial substrates has been measured at various locations in situ (Carter et al. 1985) and in artificial environments adjacent to the bay (Staver 1984, Twilley et al, 1985). For comparison with the model, reports of in-situ accumulation on natural substrates were desirable. The best data sets identified were collected from zostera marina in the lower eastern shore of the bay (Moore et al. 1994), and in Bogue Sound (Penhale 1977), a lagoon situated 300 km south of the bay. Initial parameters for epiphytes were adapted from the phytoplankton component of the CBEMP. Final parameters (Table 2) were selected to obtain reasonable agreement between computed and observed epiphyte abundance (Fig. 10).

## Components of Light Attenuation

Components of light attenuation in the water column were evaluated for each of the CBPS. Initial parameter values were derived through regression using fixed and volatile solids as independent variates and light attenuation as the dependent variate. Values were refined to improve agreement with observations. Background attenuation ranged from 0.2 to 1.5  $\text{m}^{-1}$ . Higher values were assigned at the upper ends of the mainstem and tributaries. Lowest values were assigned in the lower bay, consistent with the finding that freshwater is more colored than seawater (Kirk 1994). Application of optical models (Gallegos et al. 1990, Gallegos 1994) indicates background attenuation in the bay is approximately 0.26  $\text{m}^{-1}$ . The range of values employed here results from evaluation of attenuation in individual CBPS rather than to baywide, mean conditions. Assignment of background attenuation also reflects, to some extent, attenuation that can not be accounted for using computed solids. Attenuation by fixed and volatile solids ranged from 0.055 to 0.117  $\text{m}^2 \text{g}^{-1}$ . These values agree well with values reported for similar systems (Pennock 1985). The model does not distinguish between attenuation by algae (as chlorophyll) and attenuation by total organic matter (dry weight). Assuming that algae comprise most of the particulate organic matter and utilizing the model ratios dry weight:carbon = 2.5 and carbon:chlorophyll = 75, attenuation by volatile solids is equivalent to chlorophyll-specific attenuation of 0.01 to 0.02  $\text{m}^2 \text{mg}^{-1}$ . These values are well within reported ranges (Krause-Jensen and Sand-Jensen 1998).

## Model Application

The CBEMP was applied to the ten-year period 1985-1994. The CBEMP included Phase IV of the CBPO watershed model (Linker et al. 1996) which provided distributed loads of sediments and nutrients and the Corps=CH3D-WES hydrodynamic model (Johnson et al. 1993) which provided transport. The eutrophication model, including the SAV component, was initialized once and run continuously through the simulated period. Boundary conditions and loads were updated on a daily or monthly basis. Integration time step was 15 minutes. Output from the model was stored at ten-day increments.

## Results

### Agreement with Living-Resource Parameters

Living resource criteria for the survival and propagation of SAV in Chesapeake Bay have been identified by Batiuk et al. (1992). The investigators determined maximum light attenuation for survival of SAV at the one-meter depth to be  $2.0 \text{ m}^{-1}$  for freshwater species and  $1.5 \text{ m}^{-1}$  for saltwater species. Model results were compared to these criteria by plotting median shoot biomass in each cell for each of ten growing seasons (April - October) against median computed light attenuation. Shoot densities computed by the model clearly conform to the observed criteria (Fig. 11). Although computed SAV occasionally survives for a season under conditions that marginally exceed the criteria, the vast majority of computed biomass occurs in cells that meet the criteria. Model regions that substantially exceed the criteria never support SAV.

### Effect on Suspended Solids

The influence of SAV on suspended solids was determined by collecting suspended solids observations inside and outside SAV beds. The modeled influence was examined by performing analogous observations on the model. Computed solids in cells that supported SAV were compared to computed solids in adjacent cells outside the SAV zone. As with the observations, considerable scatter occurs in the ratio (Fig. 12). The relationship (Equation 10) employed to simulate SAV effects on solids clearly works as desired, however, and model results are in reasonable agreement with the trend exhibited by observations.

### Spatial Distribution of SAV and Light Attenuation

SAV abundance is not uniformly distributed in the bay system (Fig. 13). Within the mainstem bay and its major embayments, SAV is concentrated in CB1, near the confluence with the Susquehanna River, and in the lower half of the bay. Of the tributaries, only the tidal fresh and transitional portions of the Potomac River exhibit substantial abundance although lesser accumulations exist in the lower Rappahannock and York Rivers.

SAV abundance distribution is affected by two factors: area available for SAV growth and conditions suited for SAV growth. A goal of bay management is restoration of SAV to the Tier III level (Batiuk et al. 1992). That is, SAV should be restored to the two-meter depth contour. Using the Tier III areas as a measure of potential habitat, the observed abundance can be normalized into a mass per unit area (Fig. 14). This measure provides an indication of regions in which conditions are not suited for SAV growth. If SAV filled potential habitat in all segments, the mass per unit area would be equal in all segments. Instead, mass per unit area roughly follows the abundance distribution. That is, low abundance indicates poor conditions rather than small areas for SAV growth.

The observed distribution of SAV largely reflects the distribution of light attenuation (Fig. 15). The mainstem bay exhibits a classic turbidity maximum (Schubel 1968) that typically occurs in CB2. Lesser attenuation occurs above and downstream of the maximum. Substantial SAV abundance is restricted to these same areas above and downstream of the maximum. The major tributaries are more turbid than most of the bay and, with the exception of portions of the Potomac, do not support substantial accumulations of SAV.

Qualitatively, the model performs excellently in reproducing the spatial distribution of SAV (Fig. 13). Substantial abundance is computed in the Susquehanna Flats, in the lower bay, and in the upper Potomac River. Lesser amounts are computed in the eastern embayments (EE1, EE2), and in the lower Rappahannock

and York Rivers. Quantitatively, the median absolute difference between computed and observed abundance is 37% of the observed values, with a range from zero to more than 300%.

The model also performs excellently in capturing the turbidity maximum in the mainstem bay and the characteristic higher turbidity values in the tributaries (Fig. 15). Median absolute difference between computed and observed attenuation is  $0.19 \text{ m}^{-1}$  or 13% of the observed values.

#### Trends in SAV

Moore et al. (2000) noted a substantial increase in *ZOSTERA* abundance from the period 1985 to 1990. Abundance of the other communities was less than *ZOSTERA* and exhibited no trend. Comparison of model results with time series of observed community abundance (Fig. 16) indicates the model represents correctly the relative abundance in each community. Inter-annual variability and trends are not well represented, however. The median absolute difference between computed and observed bay-wide annual abundance, by community type, is 30% of observed values, with a range from zero to 240%.

#### Sensitivity to Nutrient and Solids Loads

Three model runs were made to examine the sensitivity of SAV to load reductions: 25% reduction in nitrogen and phosphorus loads (point-source and distributed); 25% reduction in solids loads; 25% reduction in both nutrient and solids loads. Nutrient load reductions were adapted as characteristic of present management plans which call for 20% and 35% reductions in total nitrogen and phosphorus loads, respectively (Thomann et al. 1994). No goal presently exists for solids reductions. A reduction equivalent to the nutrient reductions was assumed as a reasonable starting point. Results from the sensitivity runs were compared to a base run. The base was identical to the calibration except for initial conditions.

The base and sensitivity runs were initiated by running the model to steady-state under a set of average hydrological conditions and appropriate loads. Following equilibration, the ten-year sequence of actual hydrological conditions was simulated.

The first result of the sensitivity runs is that the greatest abundance gains occur in segments that already support substantial SAV (Fig. 17). The second is that nutrient controls alone do little to introduce SAV into areas in which it does not already occur. Solids reductions or solids combined with nutrient reductions are required to re-introduce SAV into the tidal fresh portions of the James, York, and Rappahannock Rivers. The transition regions, which contain the turbidity maxima, of four major tributaries do not support SAV under any of the sensitivity reductions. Multiple segments in the mainstem and tributaries show greater improvement from solids control than nutrient control. Almost all segments show greater improvement from combined nutrient and solids reductions than nutrient reductions alone.

An expected result of the sensitivity runs was that solids reductions alone would decrease SAV in some areas due to relaxed light limitation on epiphytes and phytoplankton. In the turbid portions of the system, the expected increase in attenuation from organic matter did occur. The beneficial effect on SAV of reduced attenuation from fixed solids more than compensated for the increased attenuation from organic matter, however. Consequently, SAV never diminished in response to solids reductions.

Sensitivity to solids reductions can be understood by examining the composition of solids in the system. Extensive solids observations, including total suspended solids, fixed solids, volatile solids, and particulate organic carbon, are available through the monitoring data base (US EPA Chesapeake Bay Program Office,

Annapolis MD). Observations of fixed and volatile solids comprise 13% of the data base. From the remaining observations, volatile solids were estimated as 2.5 times particulate organic carbon (assuming organic matter is composed of carbon, hydrogen and oxygen in the atomic ratio 1:2:1). Fixed solids were computed as the total less estimated volatile component. Fixed solids exceed volatile solids virtually throughout the system (Fig. 18). Consequently, a program that controls volatile solids, through nutrient controls, addresses only a small fraction of solids in the system.

The components of light attenuation in the system can be examined by using the modeled color, solids distributions, and epiphytes. For this analysis, a mean depth of 1 m was assumed. Conforming to the distribution of volatile and fixed solids, attenuation from fixed solids exceeds attenuation from volatile solids in almost all regions (Fig. 19). The system can be divided into two categories: regions in which attenuation from color and fixed solids exceeds attenuation from organic matter (volatile solids and epiphytes), and regions in which attenuation from organic matter exceeds attenuation from fixed solids. Since organic matter is subject to reduction via nutrient controls, this categorization also divides the system into regions that will benefit most from solids reductions versus nutrient reductions. Color and fixed solids dominate attenuation throughout the major tributaries and in the upper segments of the mainstem. Only in the lower portion of the mainstem (CB4 downwards) and in adjacent major embayments is attenuation from organic matter dominant.

The components of attenuation alone do not determine the response to nutrient and solids load reductions. Of paramount importance is the requirement to bring total attenuation below levels that support SAV. A more useful classification of the system is into regions subject to nutrient control and regions requiring solids control (Figure 20). Regions subject to nutrient control are areas that presently meet living resources criteria (Batiuk et al. 1992) and regions in which criteria can be met by reducing attenuation from organic matter. These correspond to regions in which attenuation from color and fixed solids is less than  $2 \text{ m}^{-1}$  for freshwater species and less than  $1.5 \text{ m}^{-1}$  for other species. Regions in which attenuation from color and solids exceeds  $1.5 \text{ m}^{-1}$  (saltwater) to  $2 \text{ m}^{-1}$  (freshwater) will never support SAV absent reductions in fixed solids. This classification indicates SAV cannot be restored to large portions of the major tributaries solely via nutrient reduction. Restoration of SAV to the turbidity maximum of the mainstem and to the headwaters of several minor tributaries also requires solids reductions.

## Discussion

### Management Implications

First, we must recognize that the present course of nutrient management in the bay and its watershed will benefit the system's SAV. On the scale of CBPS, abundance is projected to increase a median of 37% in response to 25% nutrient reductions (Fig. 17). These improvements occur largely in segments that already support SAV, however. Introduction of SAV to areas in which it does not presently occur, notably the tidal fresh portions of the James, Mattaponi, and Rappahannock Rivers, is possible through nutrient controls (Fig. 20). These controls must exceed the 25% range examined here, however. Through improvements in technology and control of alternate sources (e.g. atmospheric loads), nutrient reductions greater than planned under the 1987 agreement (Baliles et al. 1987) are possible. All that is required is the will to implement them.

Nutrient controls alone, however, are not sufficient to restore a system-wide distribution of SAV. Substantial portions of the major tributaries require solids reductions to support SAV (Fig. 20). Solids reductions can also be viewed as an alternative to extreme nutrient controls. Nutrient reductions of 25% alone are not sufficient to restore SAV to the tidal fresh reaches of the James, Mattaponi, and Rappahannock Rivers (Fig.

17). Solids reductions, alone or in combination with 25% nutrient reductions, are projected to support SAV in these areas, however. In viewing the role of solids in SAV restoration, it's worth noting that major declines in SAV occurred following the Tropical Storm Agnes event (Orth and Moore 1984) which introduced massive quantities of suspended solids to the system. Also, sediment accumulation rates in at least one upper bay tributary are higher now than a century or more ago (Brush 1989), suggesting that solids loads are higher at present than in historic times.

### The Model

The median error in computing annual community abundance is less than the median error in computing long-term mean abundance in individual CBPS. This statistic belies the obvious conclusion, however, that the model performs well in computing the spatial distribution of SAV (Fig. 14) but provides little information regarding inter-annual variability in abundance (Fig. 16). In the long term, the spatial distribution of SAV abundance is determined by the area suited for SAV and by environmental factors, especially light attenuation. The areas are input to the model and the spatial distribution of environmental factors can be computed with reasonable accuracy. Consequently, the spatial distribution of SAV abundance can be computed with corresponding accuracy.

Inter-annual variability in SAV abundance is affected by a host of factors. These include environmental influences that vary on numerous time scales and inherent properties of the biota. Short-term or localized events such as storm pulses can have a significant impact on SAV (Moore et al. 1997). Consistent, universal simulation of event-scale processes is currently beyond the capability of the CBEMP. Moreover, the response of the plants to events must also be represented. Consequently, improvements in computing year-to-year variability await both more accurate environmental models and improved representations of plant physiology.

A high priority for model improvement should be placed on models of plant propagation. This includes local propagation via roots and rhizomes and propagation over distances via seeds and plant fragments. The present model assumes a trace, refuge, population in each cell that is available for growth when conditions are favorable. In reality, change in the spatial extent of existing beds is limited by the rates of production and demise of plants at the edges of the beds. The appearance of SAV in new areas, depends on the transport of viable plant material or propagules to these areas. The ability to model year-to-year variation in abundance partially depends on the ability to model propagation as well as the ability to model the environment.

Lastly, the ability to model SAV on a sub-grid scale should be attained. One feasible approach is to divide the model cell into smaller SAV cells. Since bathymetry and other measures may not be available on the desired scale and since CBEMP computations are not available on the sub-grid scale, properties of the SAV cells could be distributed randomly with mean properties determined by the larger model. A second, more advanced approach would be to develop individual-based models of plants and propagate these within model cells.

### **Acknowledgments**

This work would not have been possible without the Bay community scientists who generously contributed their time, advice, and unpublished data. These individuals include Peter Bergstrom, US Fish and Wildlife Service; Virginia Carter, US Geological Survey; W. Michael Kemp, Horn Point Environmental Laboratory; Chris Madden, South Florida Water Management District; Nancy Rybicki, US Geological Survey; and Richard Wetzel, Virginia Institute of Marine Science.

Development of the Chesapeake Bay Environmental Model Package was funded by the Baltimore District, US Army Corps of Engineers, and by the Chesapeake Bay Program Office, Region III, US Environmental Protection Agency. Permission was granted by the Chief of Engineers to publish this information.

## Figure Captions

Figure 1. SAV model state variables (boxes) and mass flows (arrows).

Figure 2. Epiphytic dry weight versus viable carbon. Staver's data from  $A_{control}$  and  $A_{low}$  ponds. Carbon obtained from chlorophyll measures using carbon-to-chlorophyll ratio of 75. Trend indicates a 15:1 ratio.

Figure 3. Ratio of suspended solids in vegetated areas to suspended solids in adjacent non-vegetated areas. Trend determined by visual comparison with observations.

Figure 4. Truncation error, coverage, and patchiness. Truncation error =  $Area(ABCD)/Area(A-B-C-D)$ . Coverage =  $Area(ABEF)/Area(ABCD)$ . Patchiness =  $Area(plants)/Area(ABEF)$ .

Figure 5. Chesapeake Bay Program Segments

Figure 6. Distribution of SAV community types.

Figure 7. Modeled (mean and interval encompassing 95% of computations) and observed (mean and 95% confidence interval) ZOSTERA shoot (A) and root (B) biomass. Shoot observations from Moore et al. 1999. Root observations assembled from Moore et alia sources. Model results from CBPS WE4.

Figure 8. Modeled (mean and interval encompassing 95% of computations) and observed (mean and 95% confidence interval) RUPPIA shoot biomass. Observations from Moore et al. 1999. Model results from CBPS EE1.

Figure 9. Modeled (mean and interval encompassing 95% of computations) and observed (mean and 95% confidence interval) FRESHWATER community shoot biomass. Observations from Moore et al. 1999. Model results from CBPS CB1.

Figure 10. Modeled (mean and interval encompassing 95% of computations) and observed biomass of epiphytes on ZOSTERA. Model results from CBPS CB7.

Figure 11. Computed shoot biomass versus light attenuation for (a) FRESHWATER community, (b) RUPPIA, and (c) ZOSTERA. Each point represents seasonal median value in one model cell. Dashed line indicates living-resource criteria for survival at one-meter depth.

Figure 12. Modeled ratio of suspended solids in vegetated areas to suspended solids in adjacent non-vegetated areas for three CBPS. Trend determined by visual comparison with observations.

Figure 13. Observed and computed mean abundance, April-October 1985-1994.

Figure 14. Observed mean abundance, April-October 1985-1994, normalized by Tier III areas.

Figure 15. Observed and computed median light attenuation at 27 stations in the bay system, April-October 1985-1994.

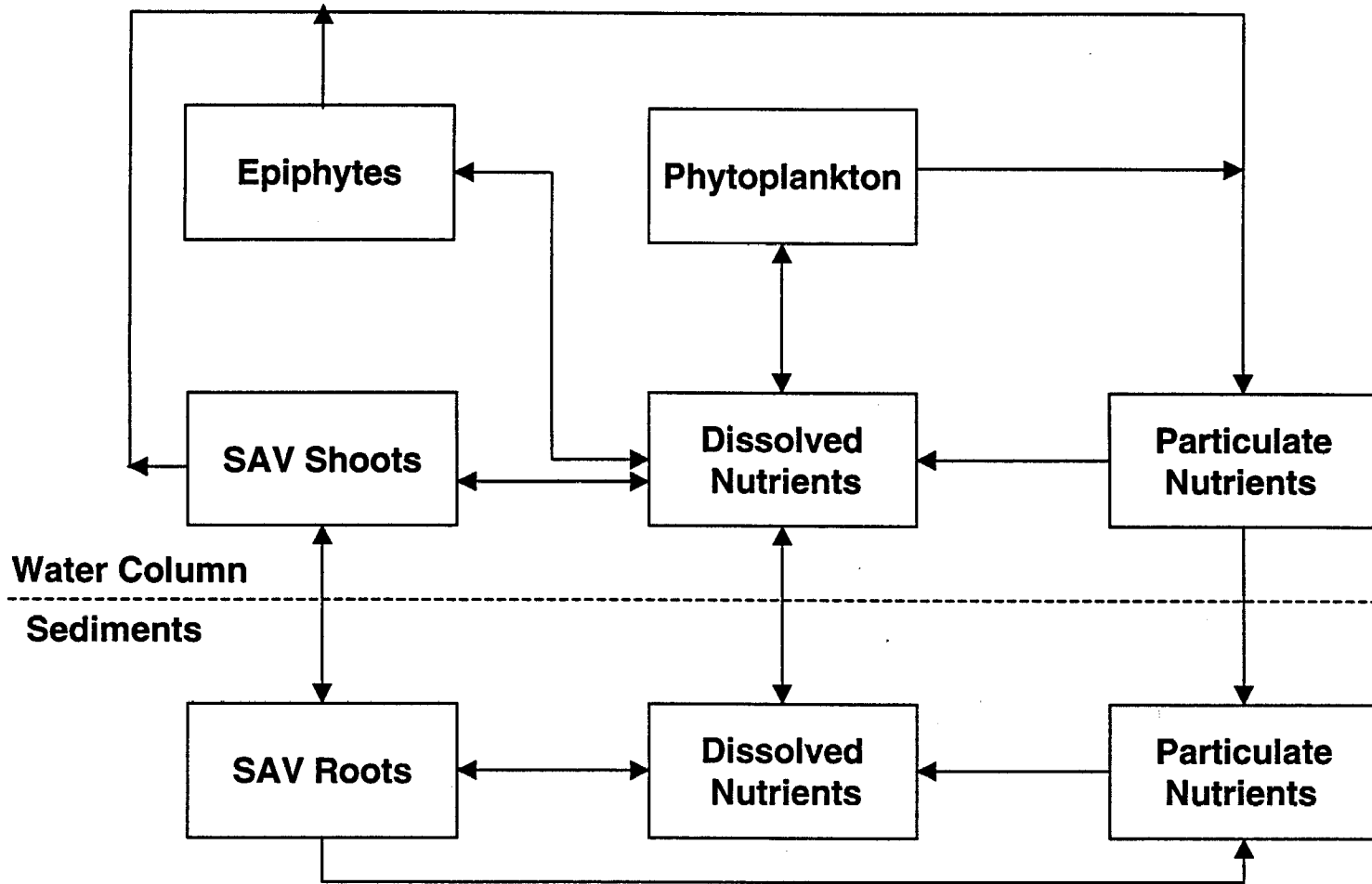
Figure 16. Observed and computed maximum abundance, by community type, 1985-1994.

Figure 17. Ten-year mean abundance increase in response to load reductions.

Figure 18. Fixed and volatile fractions of observed total solids concentration, April-October 1985-1994.

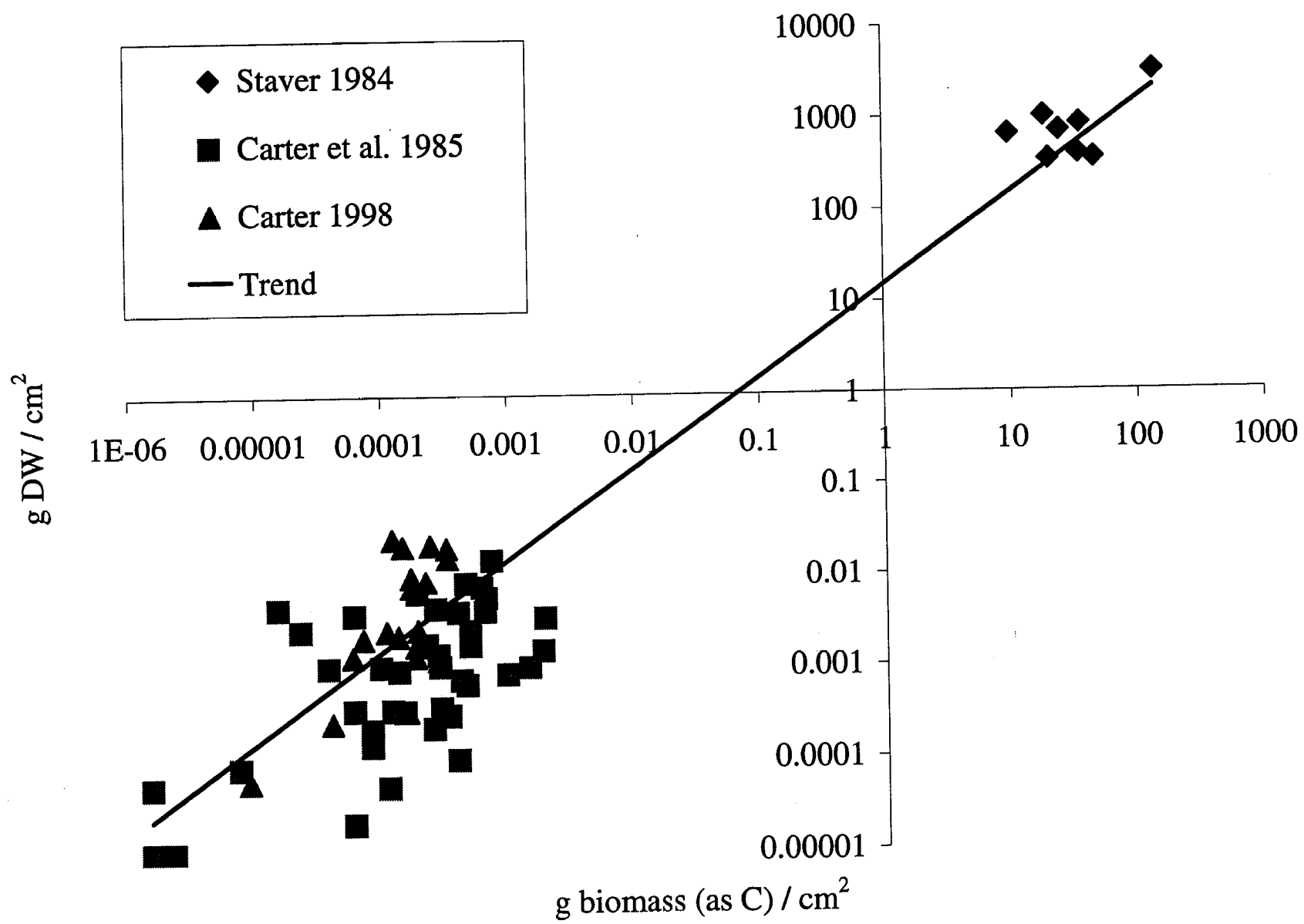
Figure 19. Modeled components of light attenuation at one-meter depth

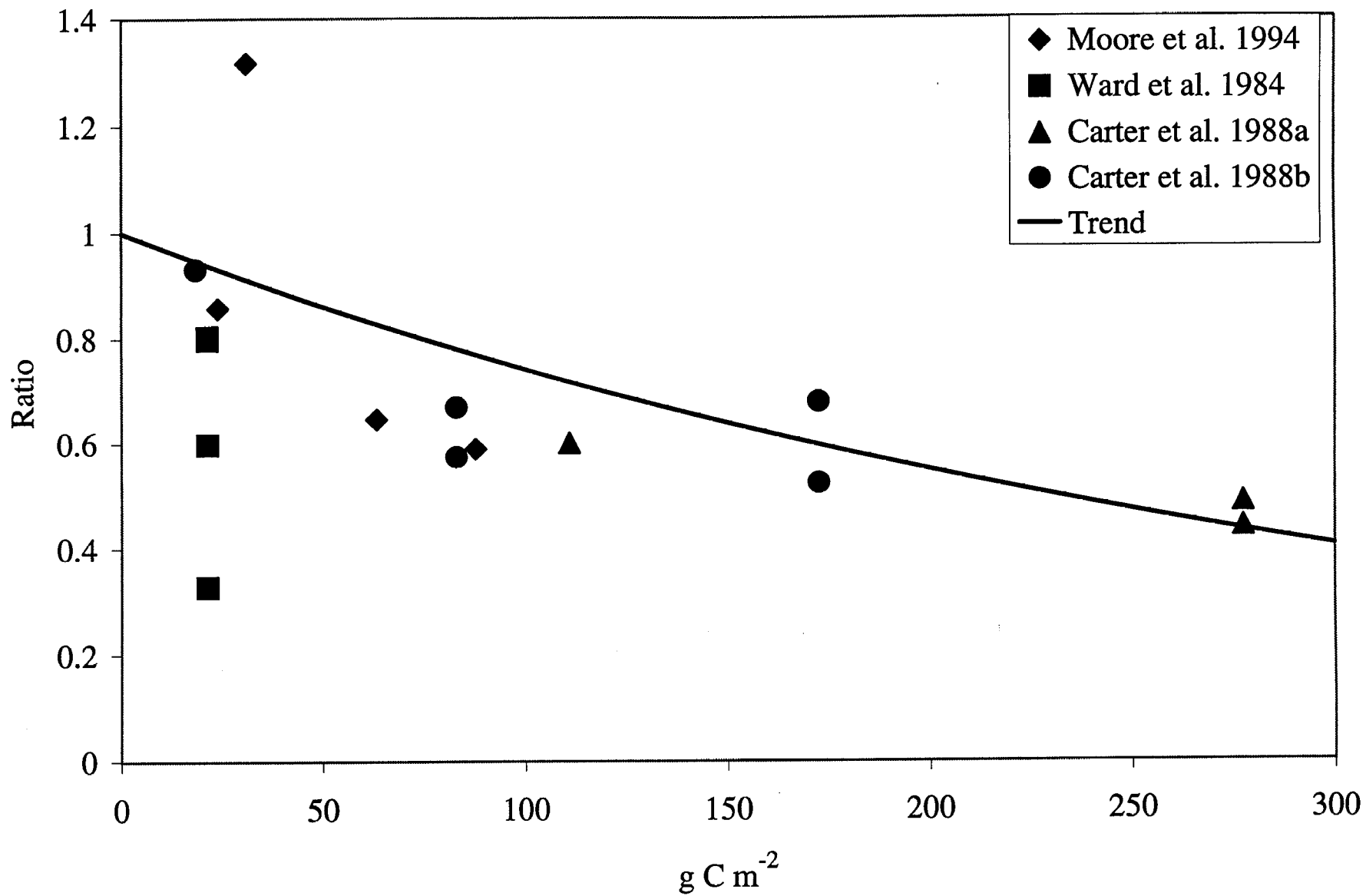
Figure 20. Regions subject to nutrient control versus regions requiring solids control.



1

11-

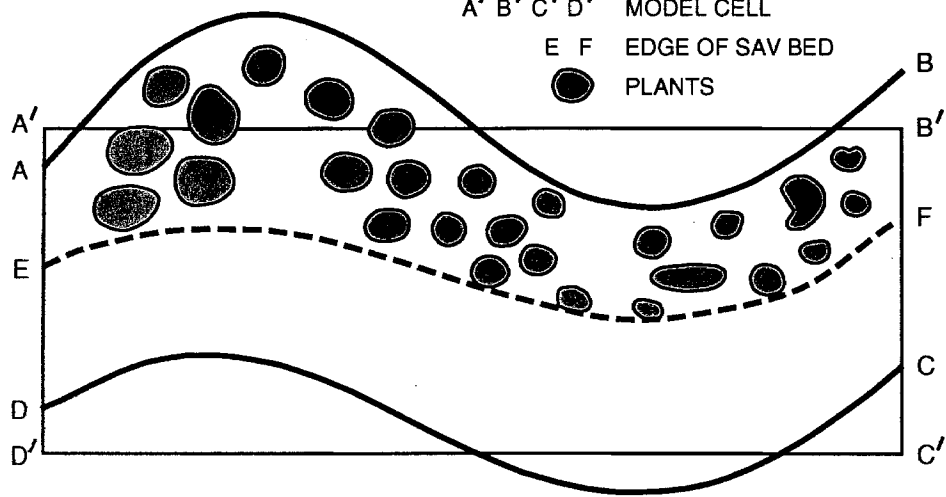


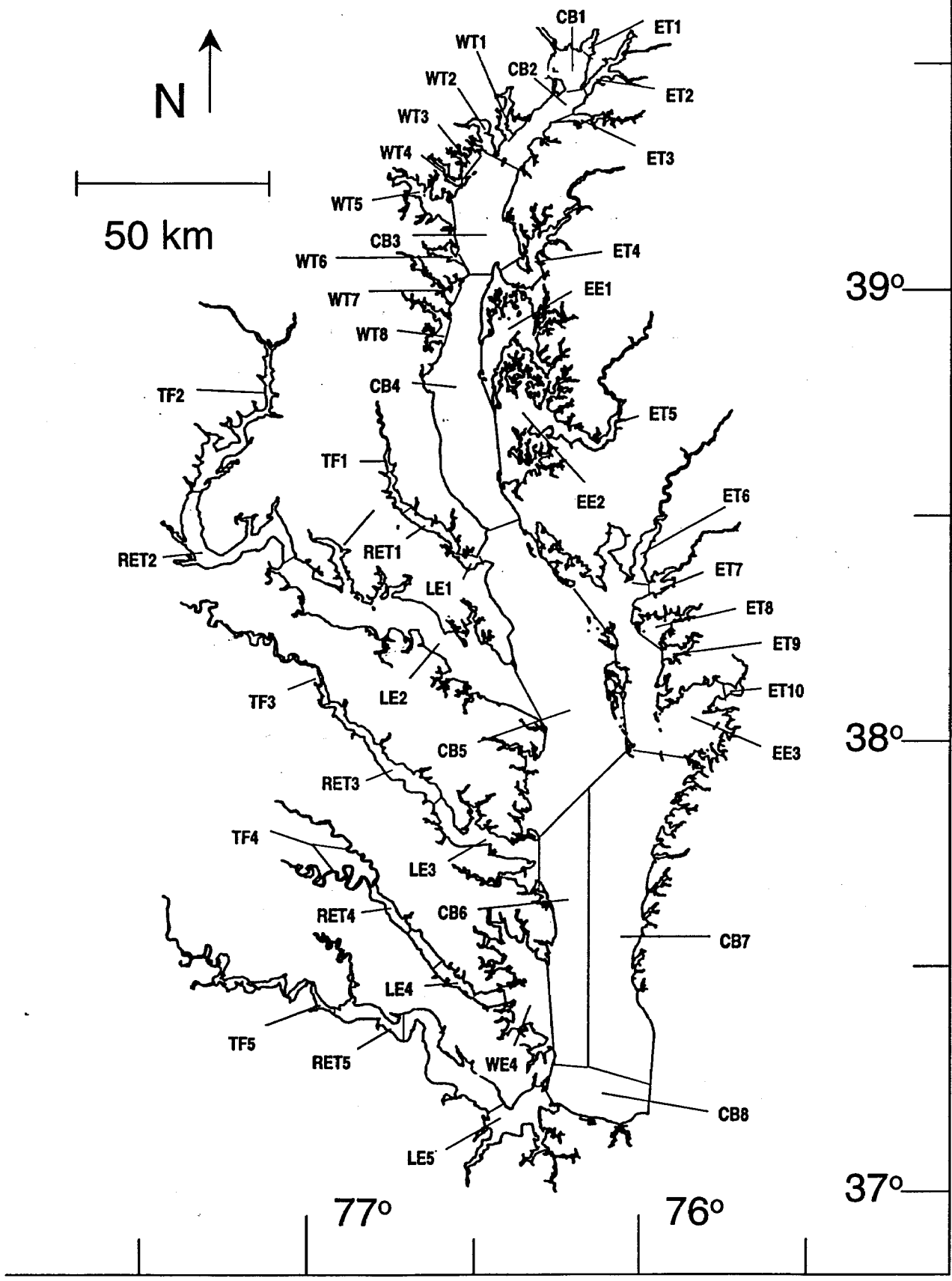


llw

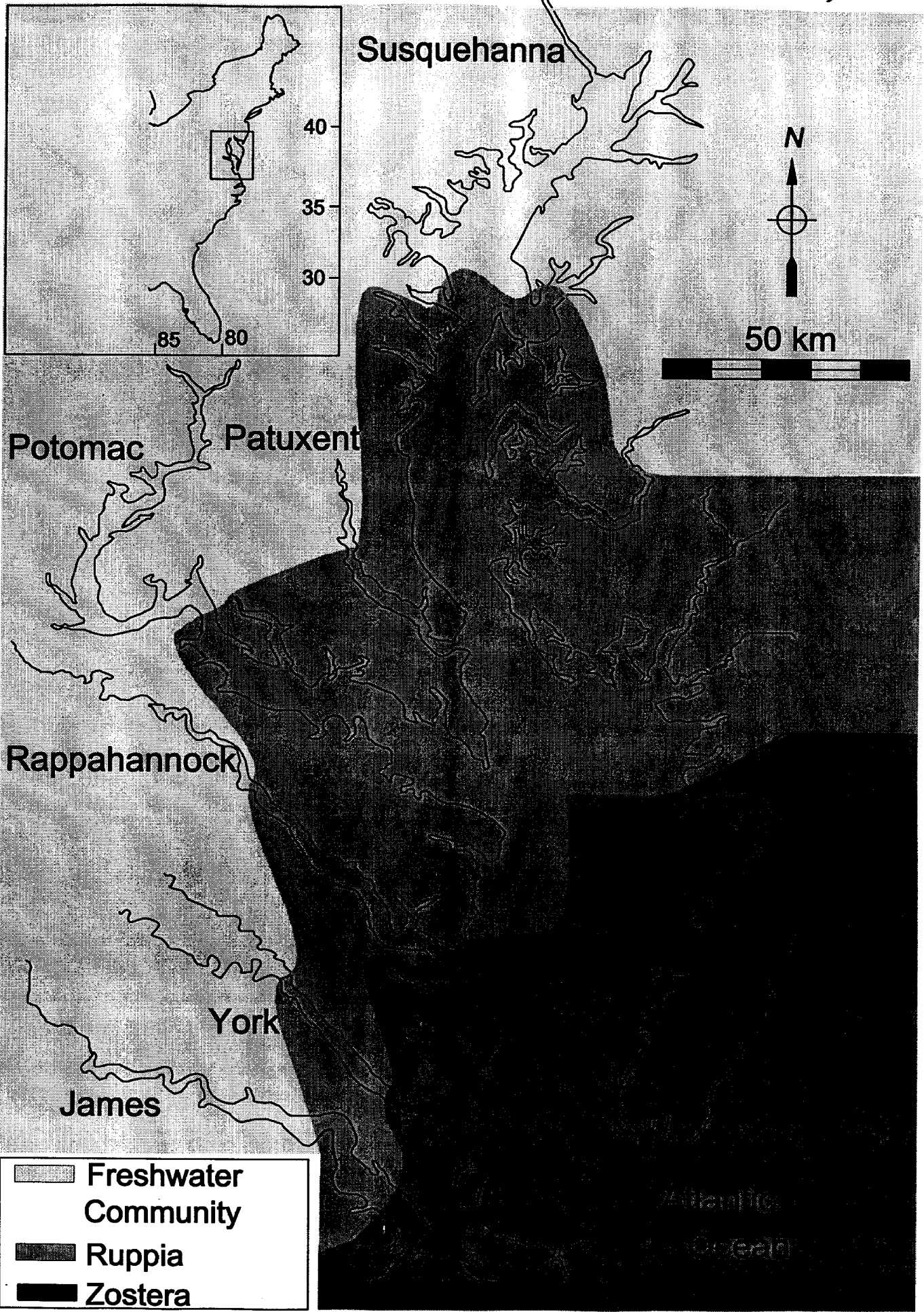
LEGEND

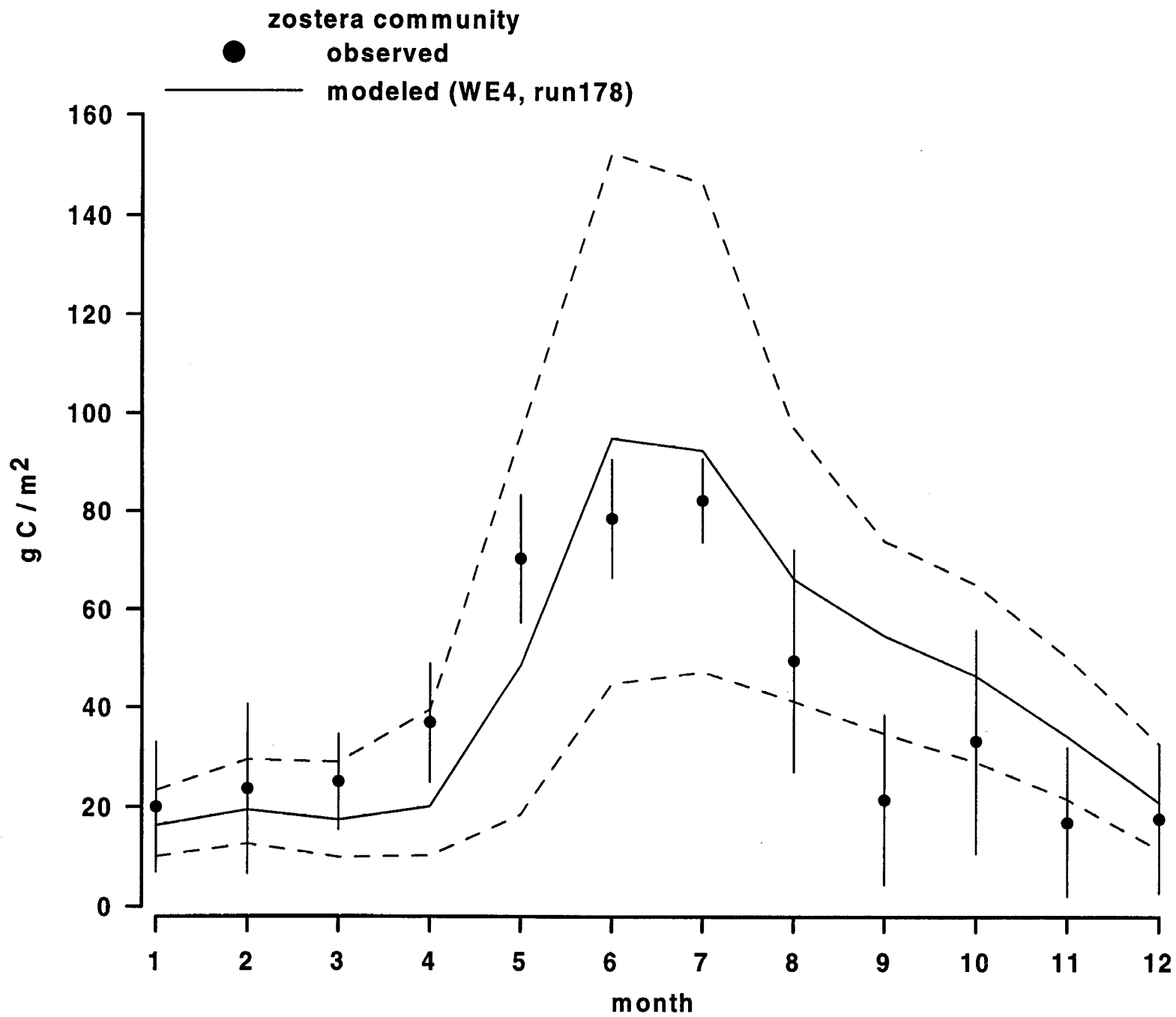
- A B SHORELINE
- C D 2 M CONTOUR
- A' B' C' D' MODEL CELL
- E F EDGE OF SAV BED
- PLANTS



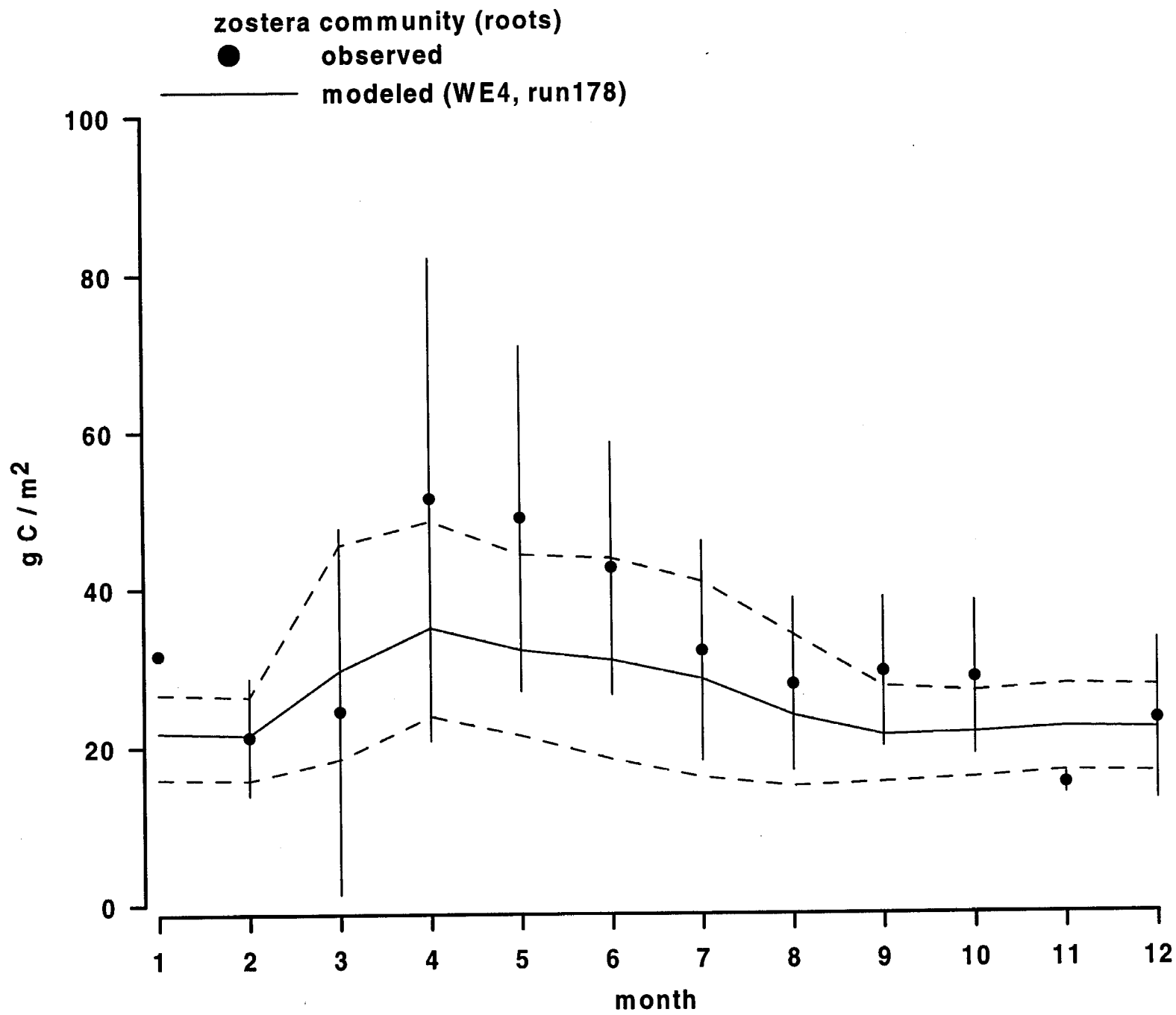


6/1

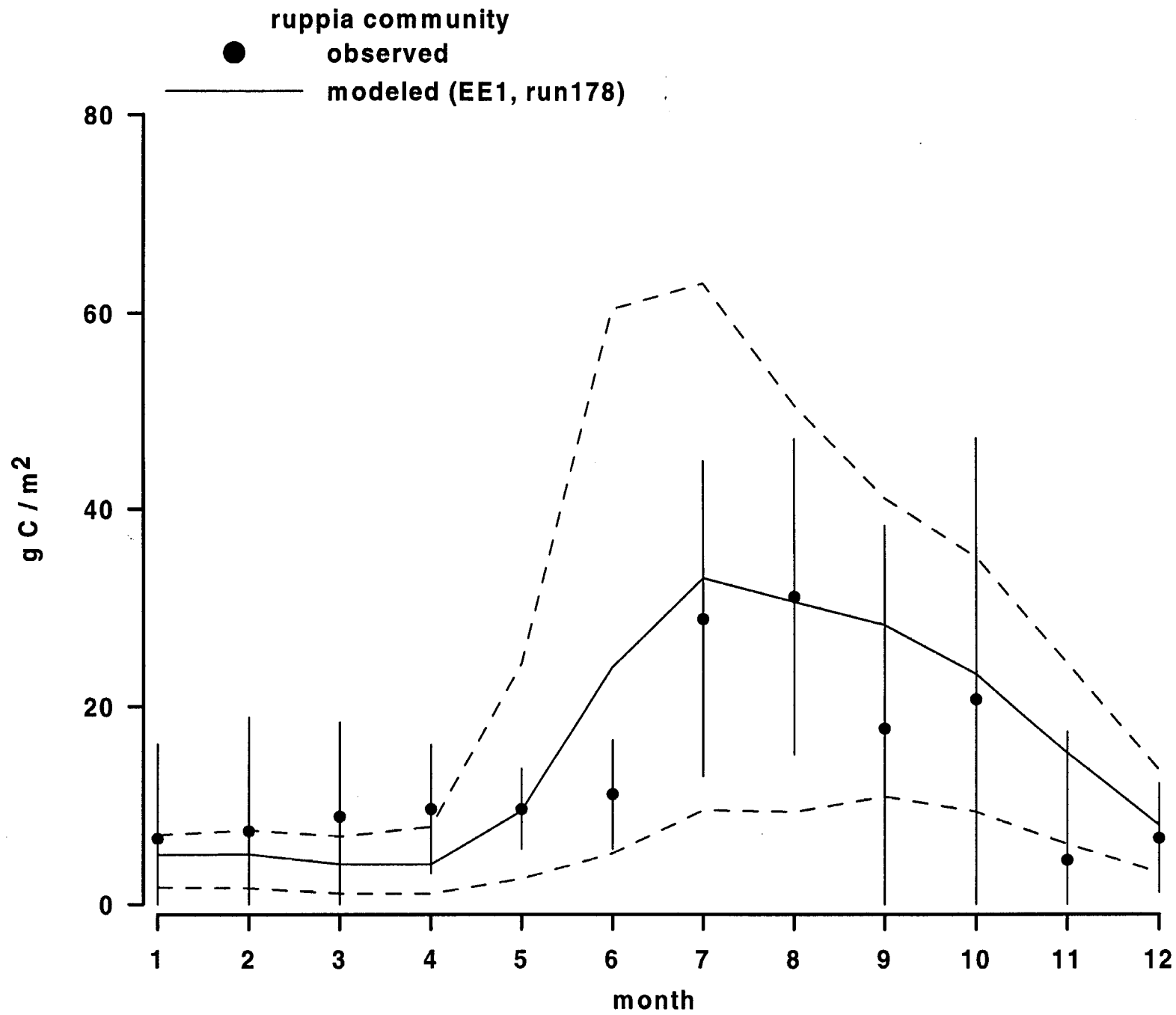




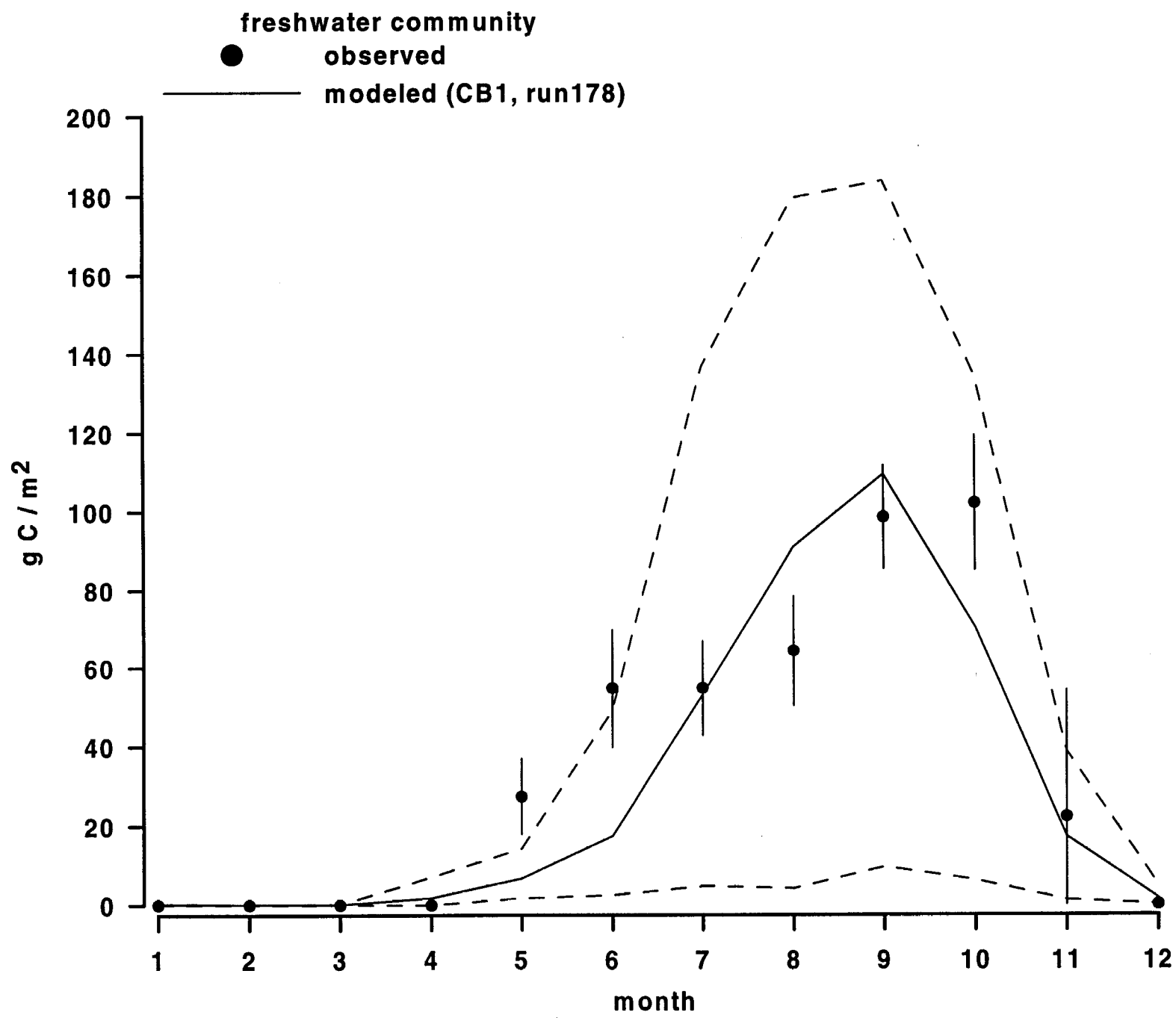
11  
A



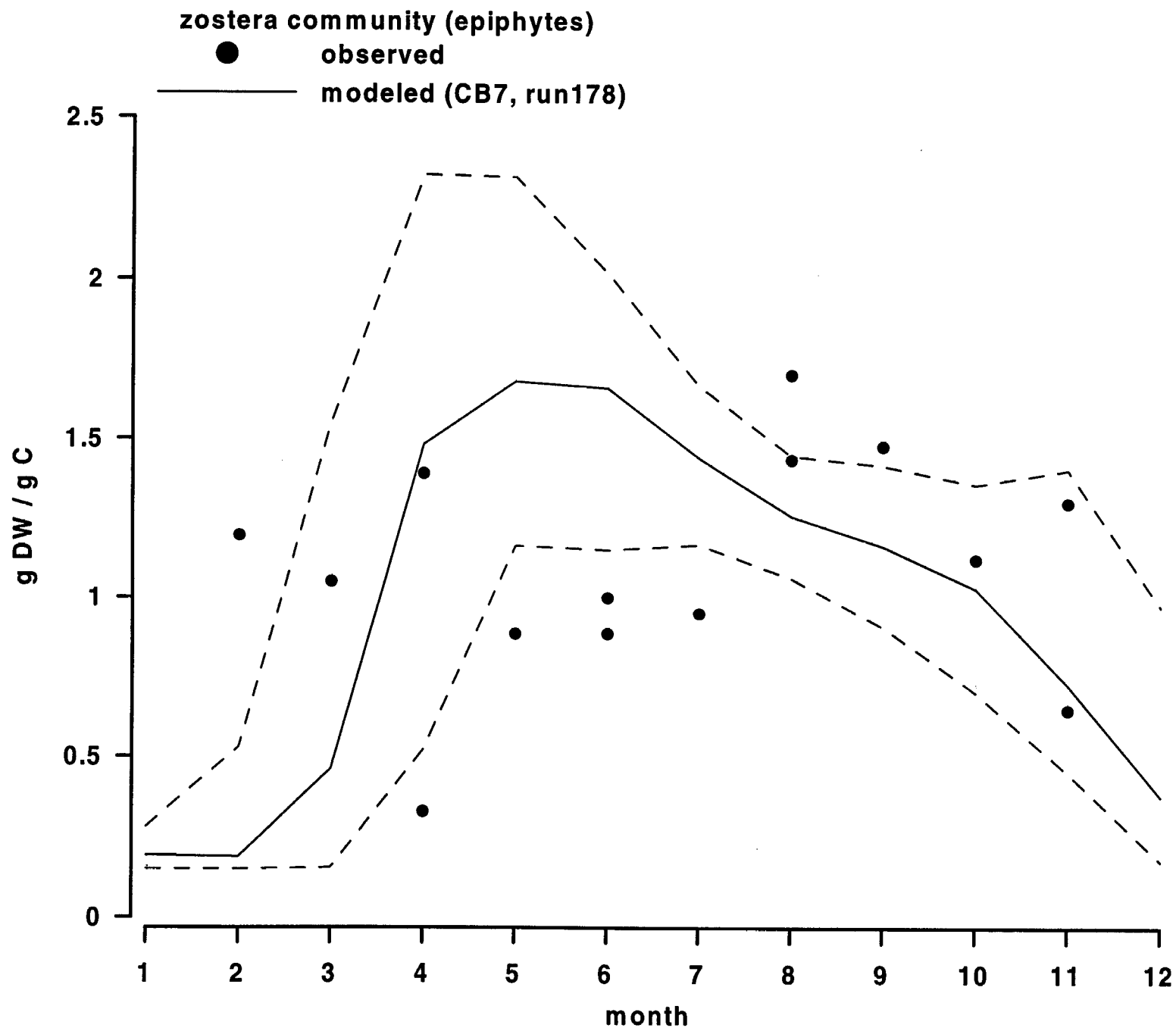
11  
6



118

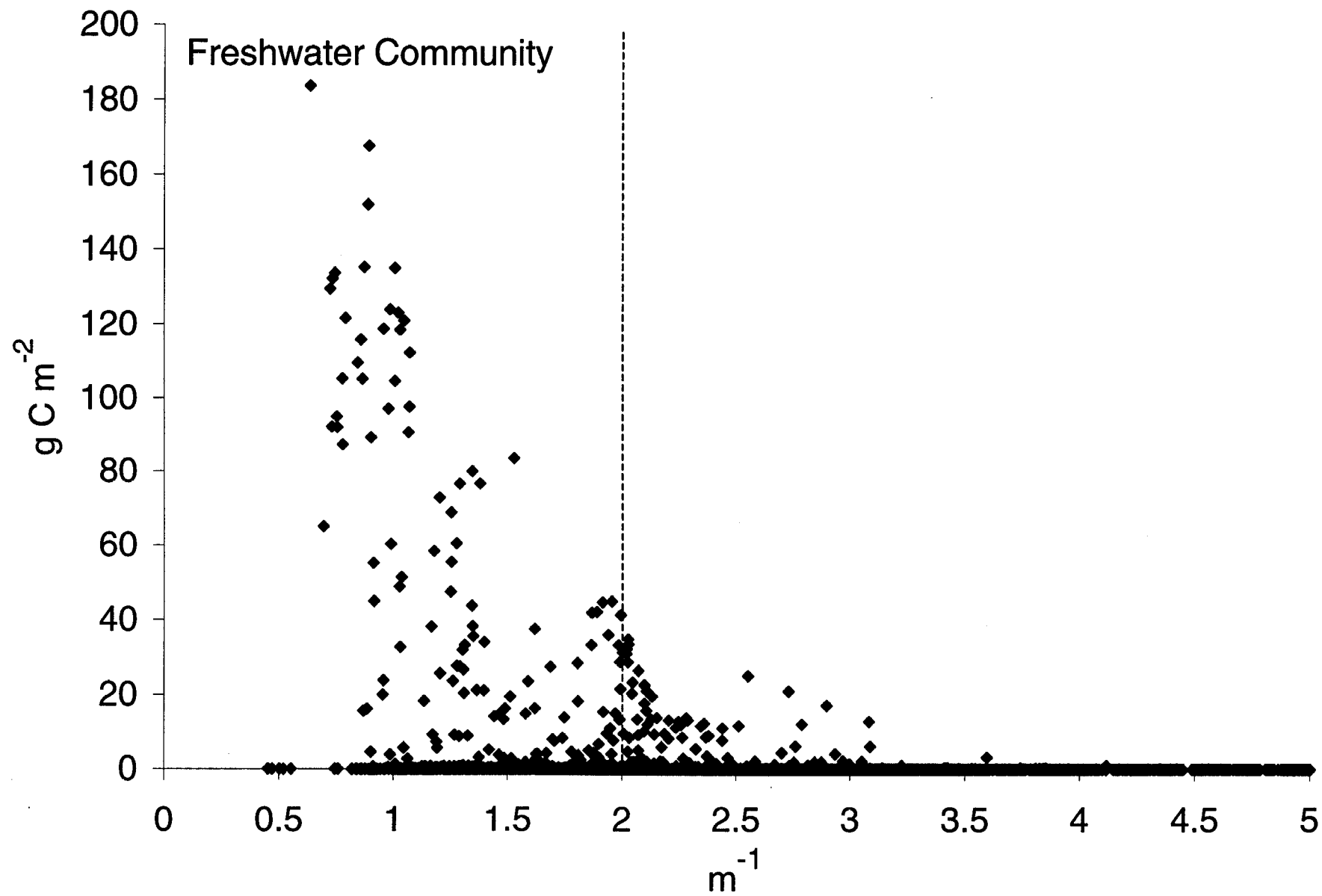


11-0



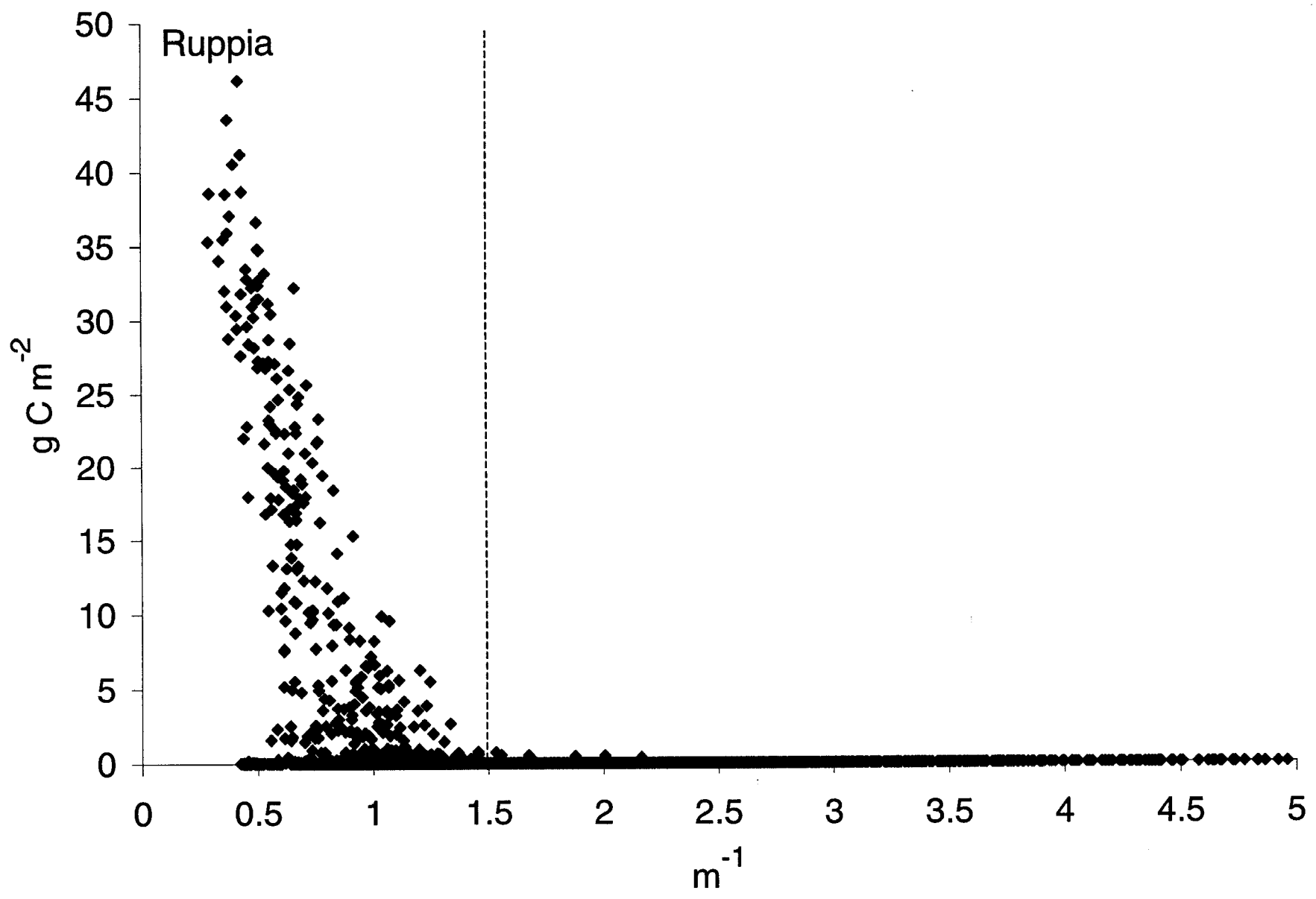
110

11a

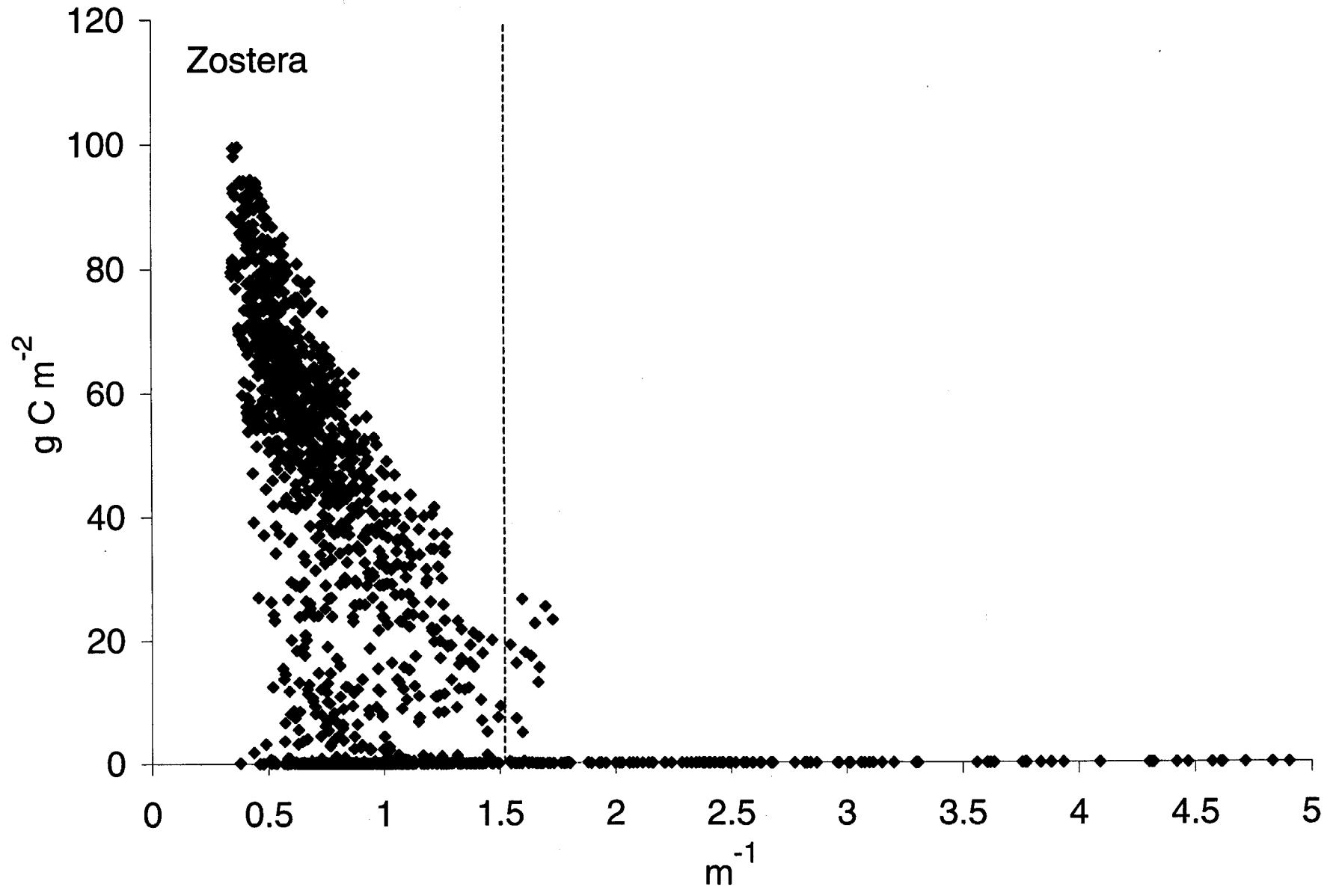


11a

11b

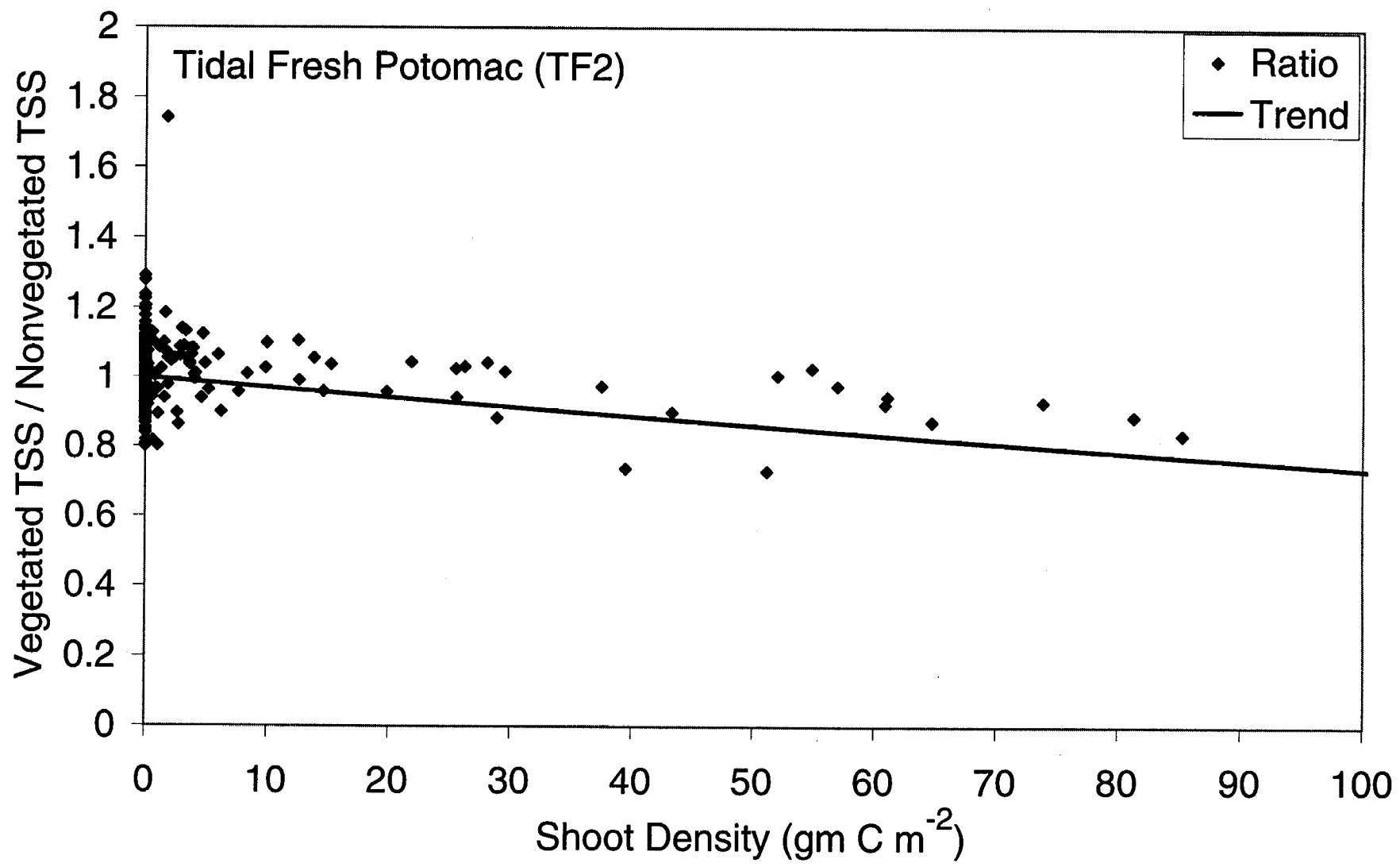


11b

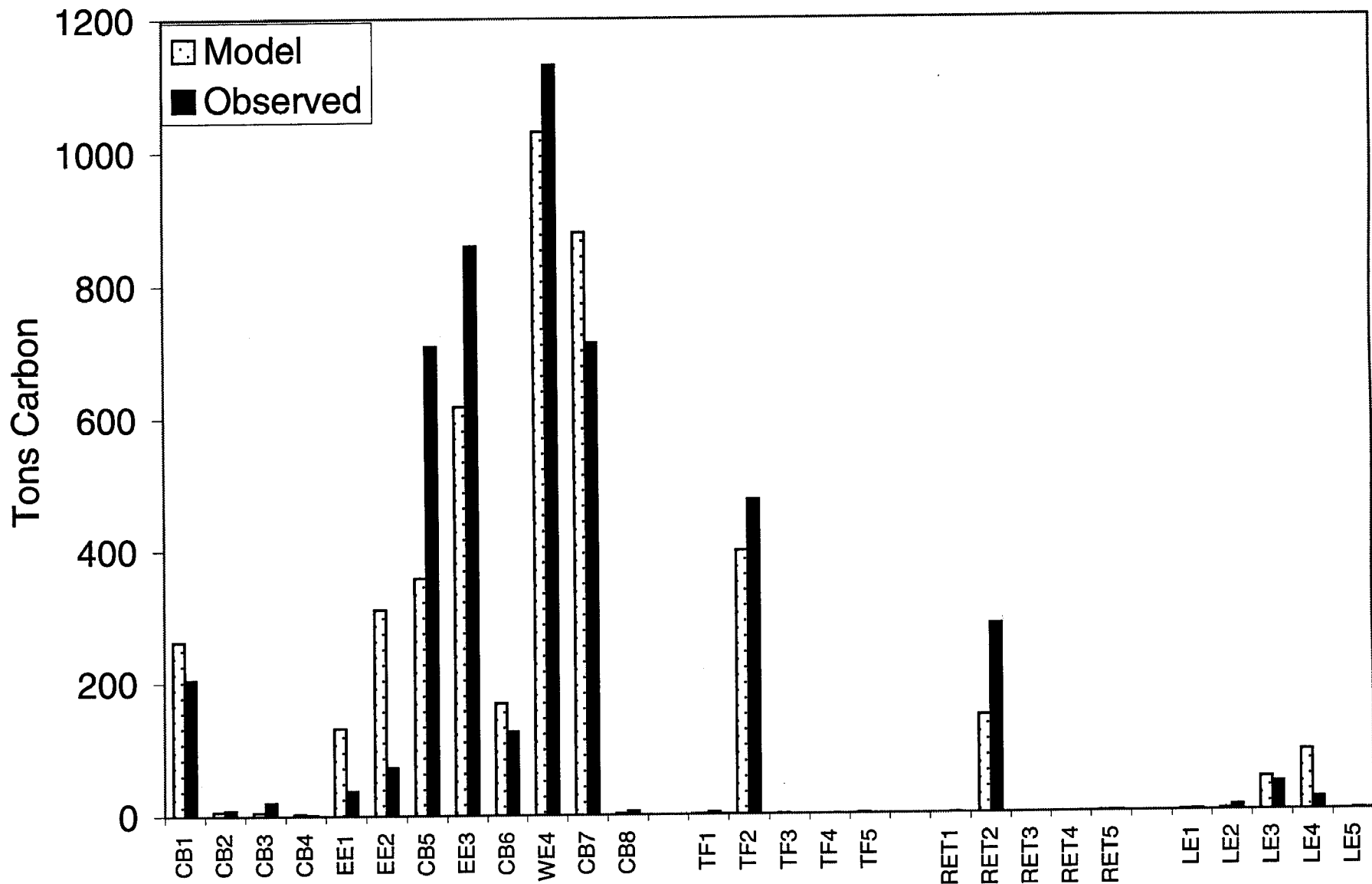


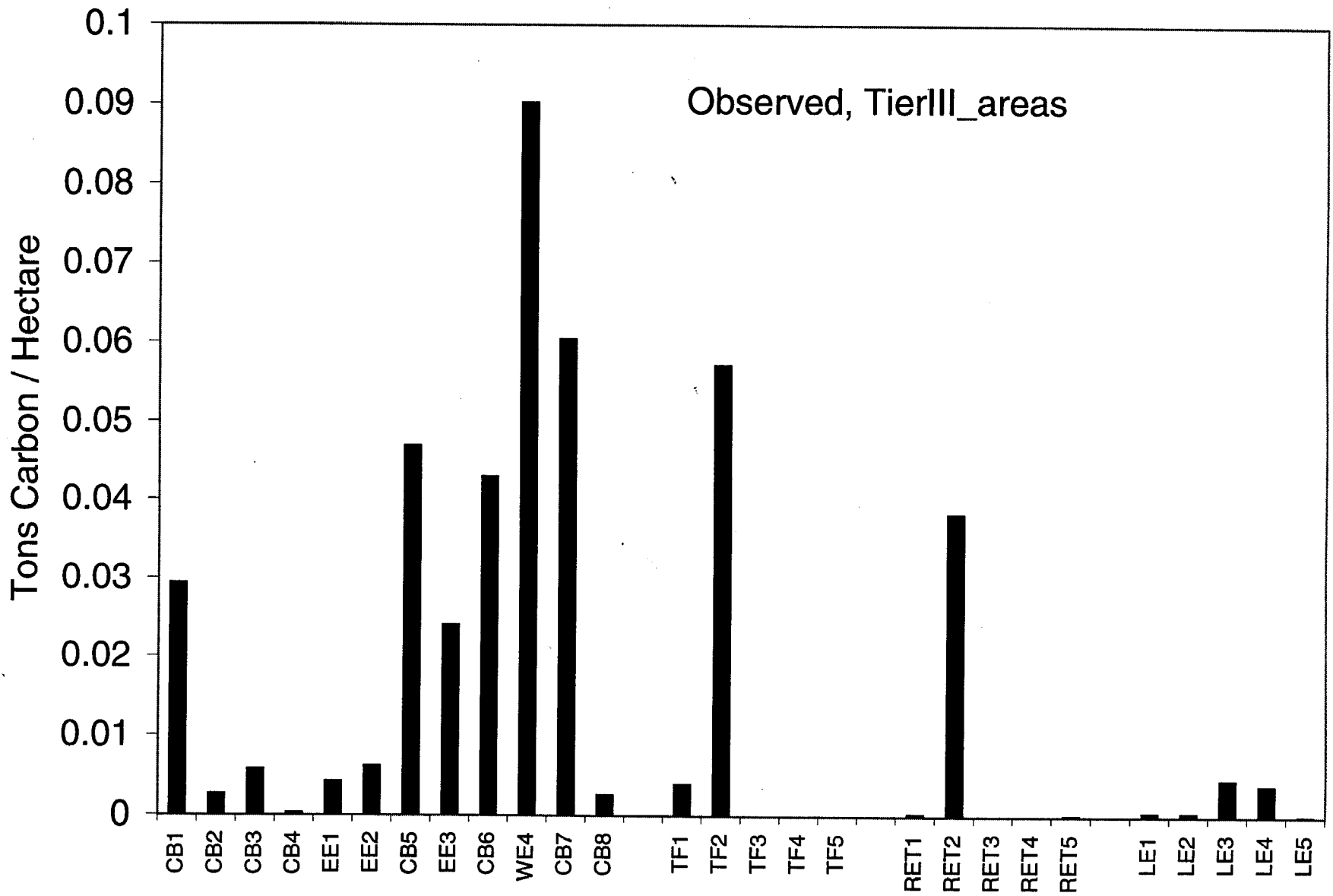
11c

12a

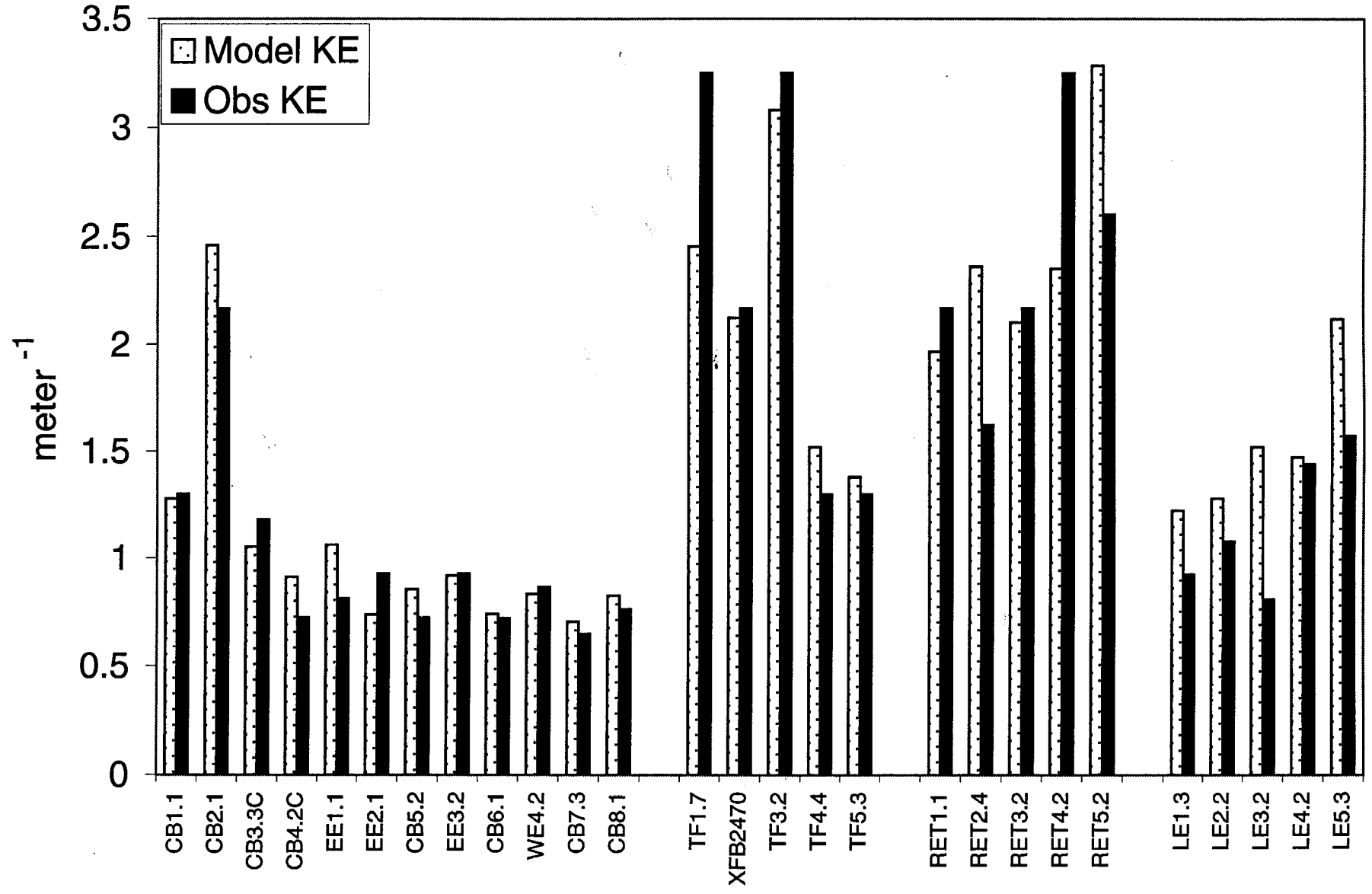


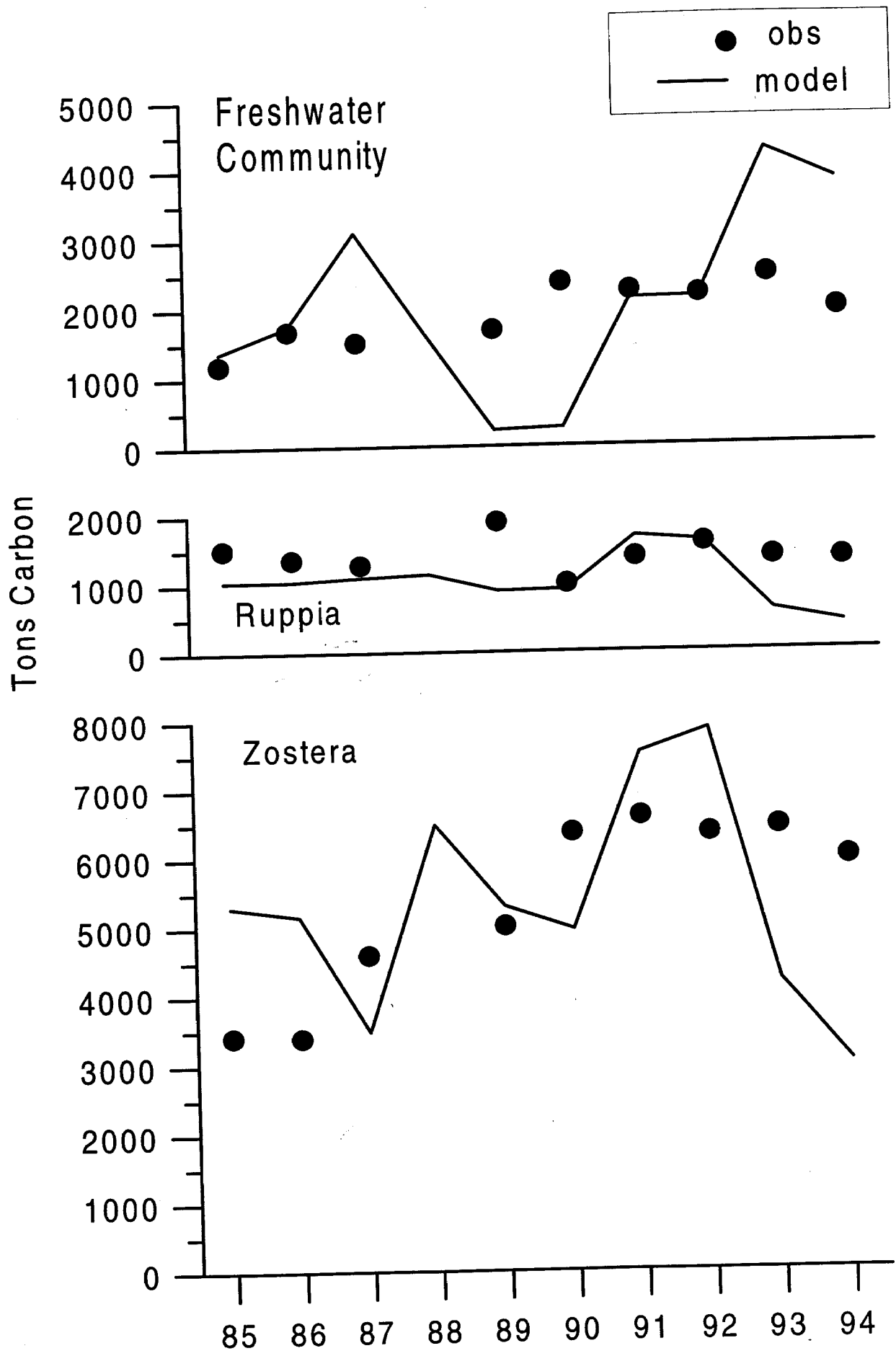
12A

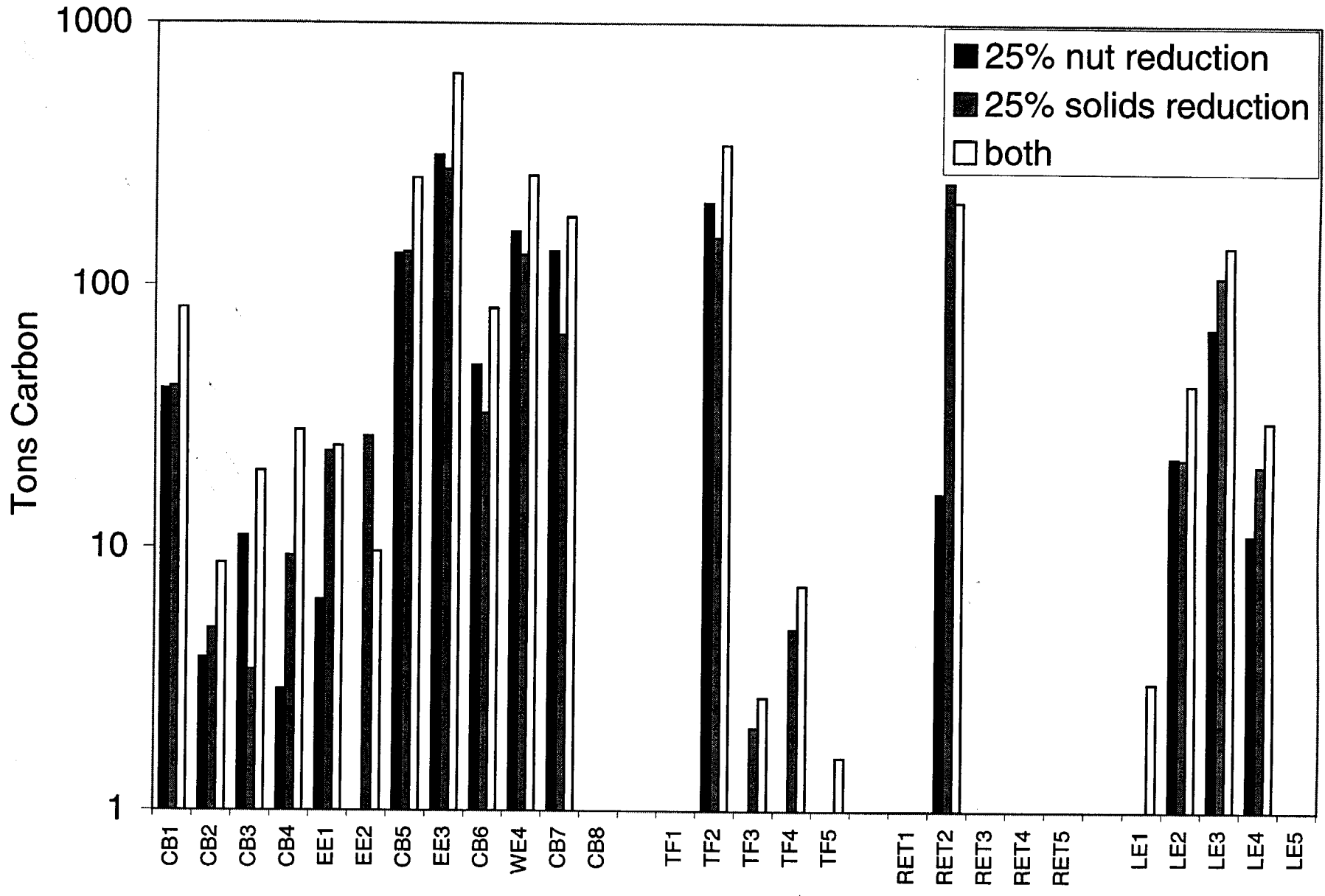


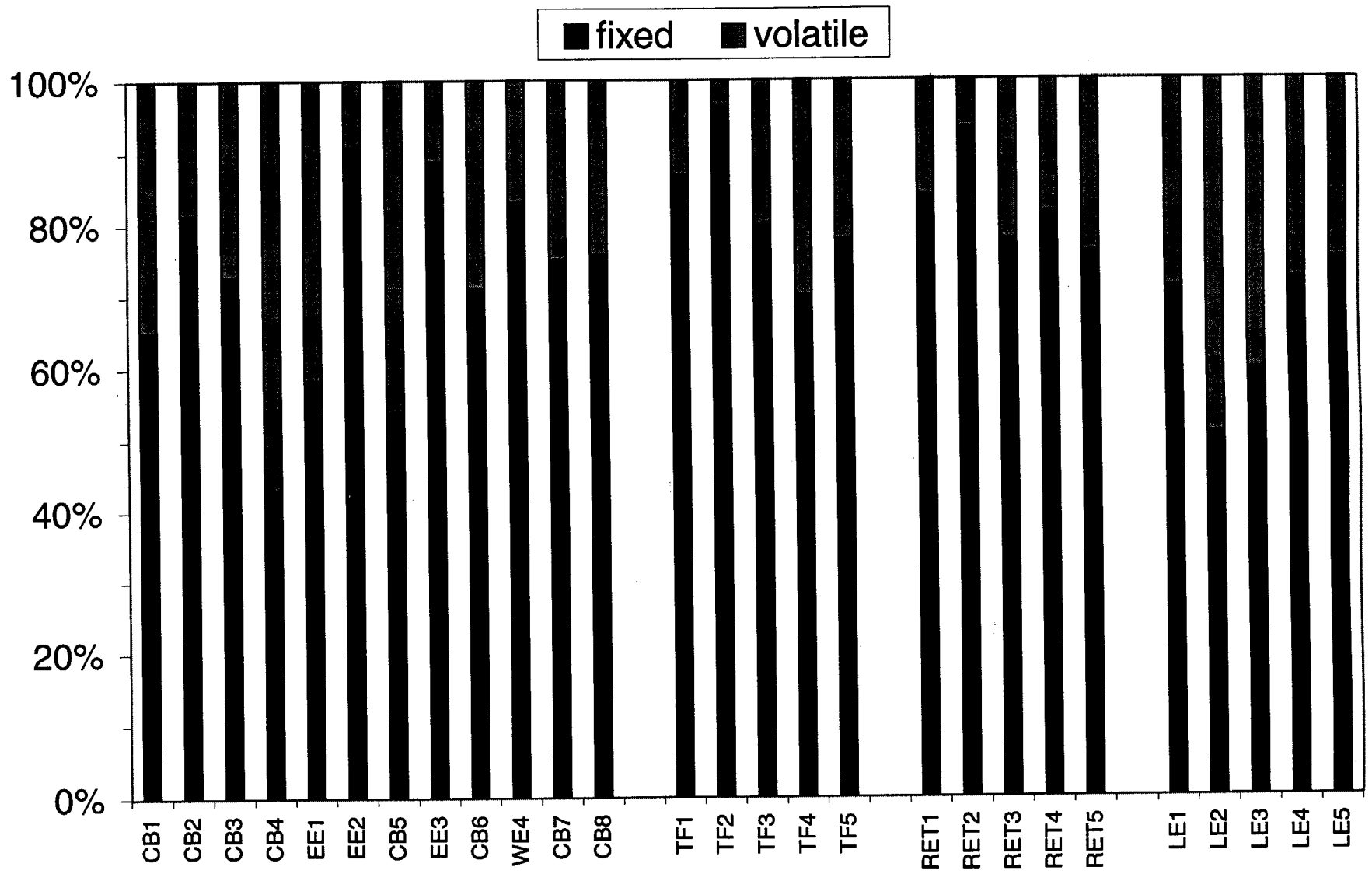


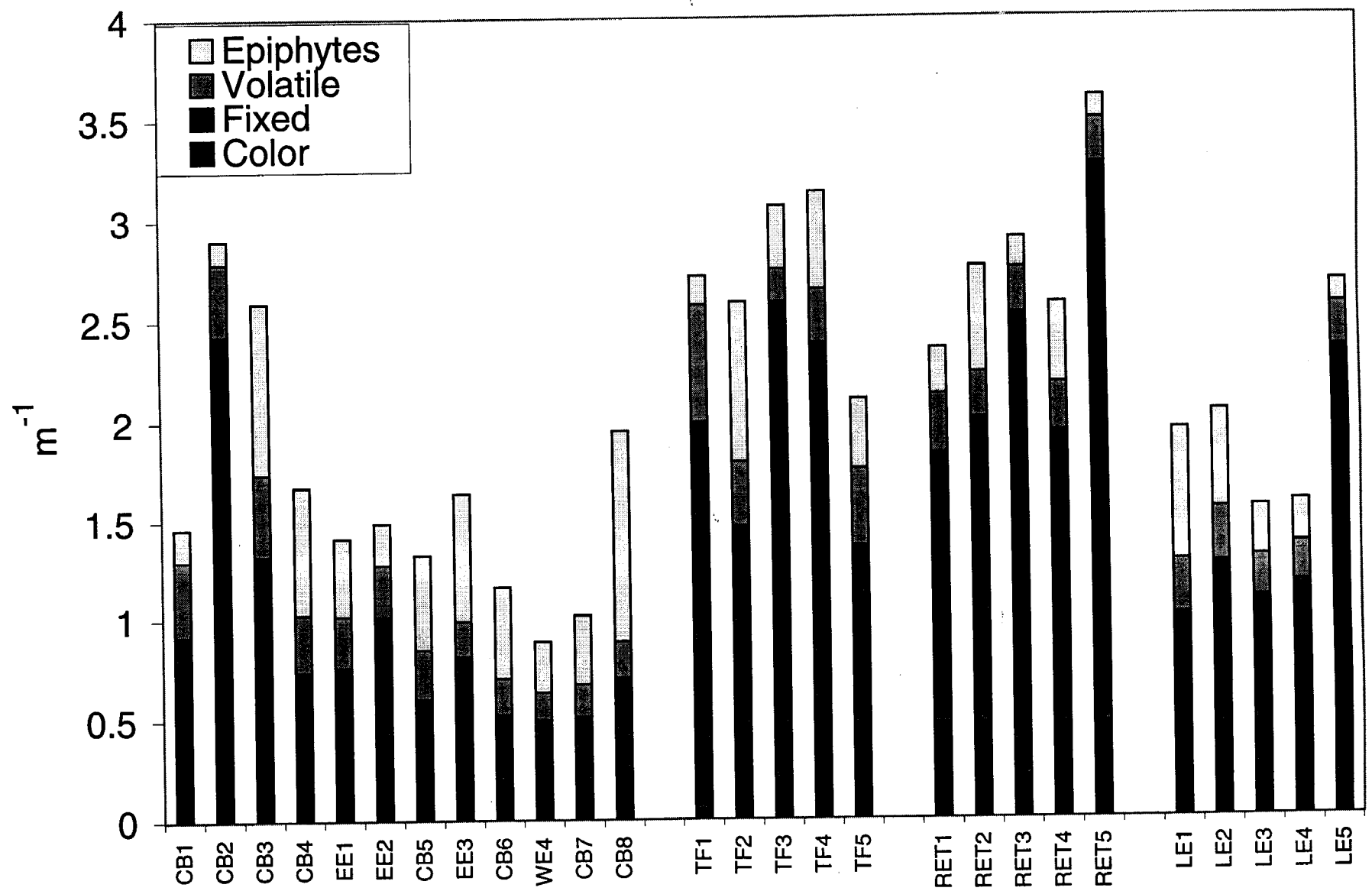
///  
F1

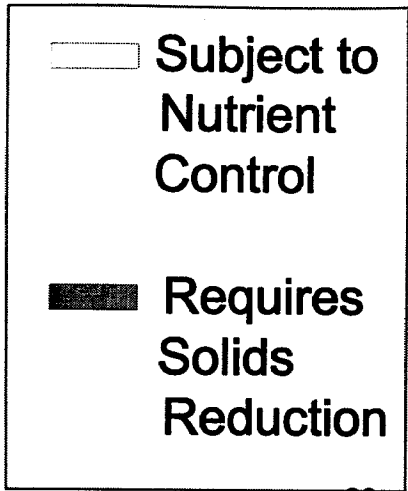












20

Susquehanna



50 km



,85 ,80

Potomac

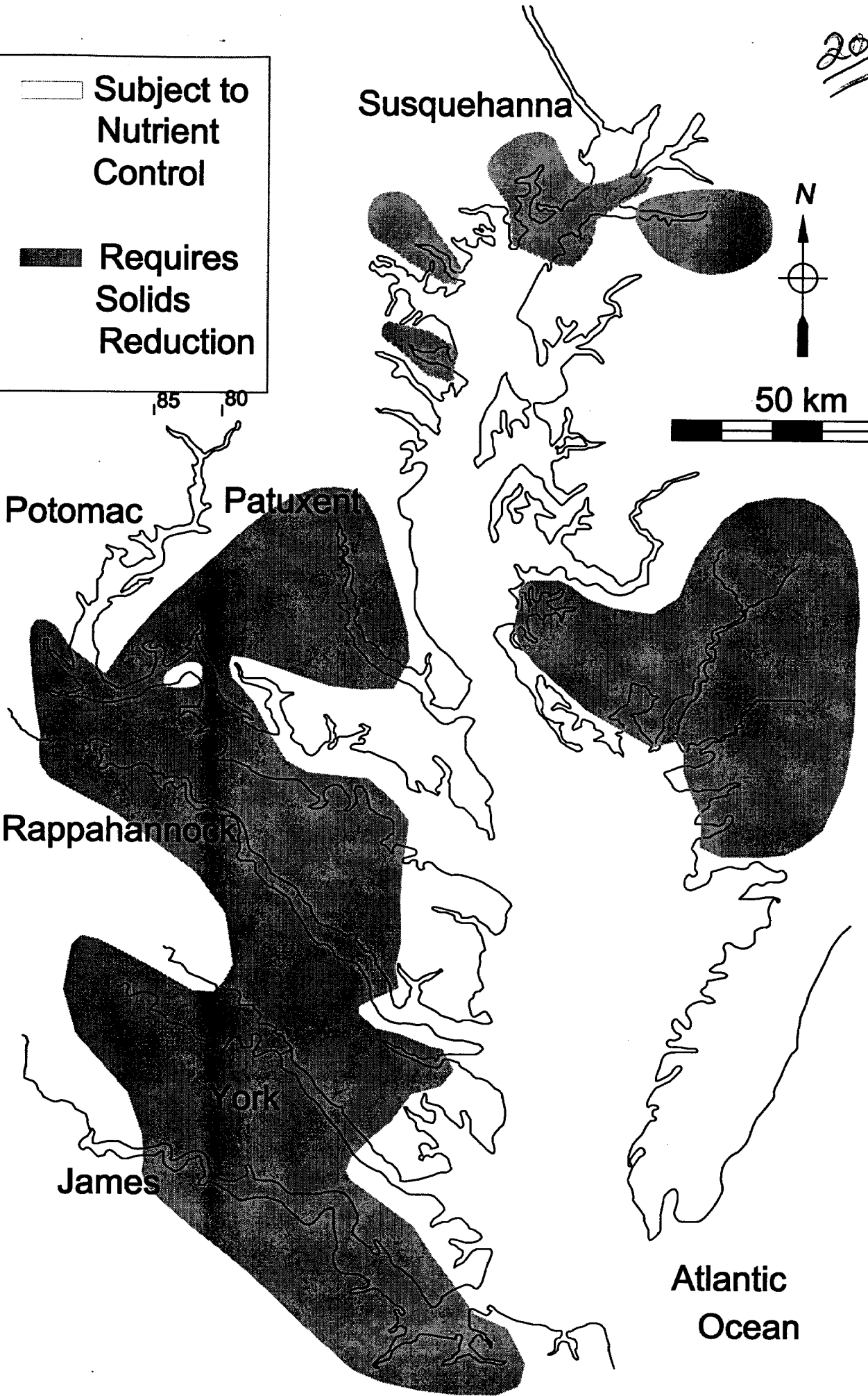
Patuxent

Rappahannock

York

James

Atlantic Ocean



## Literature Cited

- Baliles, G., Schaefer, W., Casey, R., Thomas, L., Barry, M., and Cole, K. 1987. Chesapeake Bay Agreement, United States Environmental Protection Agency Chesapeake Bay Program, Annapolis MD.
- Barko, J., and Smart, M. 1981. Comparative influences of light and temperature on the growth and metabolism of selected freshwater macrophytes. Ecological Monographs, 51(2):219-235
- Batiuk, R., Orth, R., Moore, K., Dennison, W., Stevenson, J., Staver, L., Carter, V., Rybicki, N., Hickman, R., Kollar, S., Bieber, S., and Heasley, P. 1992. Chesapeake Bay submerged aquatic vegetation habitat requirements and restoration targets: A technical synthesis. CBP/TRS 83/92, United States Environmental Protection Agency Chesapeake Bay Program, Annapolis MD.
- Borum, J. 1985. Development of epiphytic communities on eelgrass (*Zostera marina*) along a nutrient gradient in a Danish estuary. Marine Biology, 87:211-218
- Bowes, G., Van, T., Garard, L., and Haller, W. 1977. Adaptation to low light levels by hydrilla. Journal of Aquatic Plant Management, 15:32-35
- Bowes, G., Holaday, A., and Haller, W. 1979. Seasonal variation in the biomass, tuber density, and photosynthetic metabolism of hydrilla in three Florida lakes. Journal of Aquatic Plant Management, 17:61-65
- Brush, G. 1989. Rates and patterns of estuarine sediment accumulation. Limnology and Oceanography, 34(7):1235-1246.
- Carter, V., Paschal, J., and Bartow, N. 1985. Distribution and abundance of submersed aquatic vegetation in the tidal Potomac River and estuary, Maryland and Virginia, May 1978 to November 1981, United States Geological Survey Water-Supply Paper 2234-A, US Geological Survey, Alexandria VA.
- Carter, V., Barko, J., Godshalk, G, and Rybicki, N. 1988a. Effects of submersed macrophytes on water quality in the tidal Potomac River, Maryland. Journal of Freshwater Ecology 4(4):493-501
- Carter, V., Rybicki, N., Jones, R, Barko, J., Dresler, P, Hickman, R, and Anderson, R. 1988b. Data on physical, chemical, and biological characteristics of hydrilla beds, mixed vegetation beds, and unvegetated sites in the Tidal Potomac River, 1987, United States Geological Survey Open File Report 88-709, US Geological Survey, Alexandria VA..
- Cercos, C., and Meyers, M. 2000. Tributary refinements to the Chesapeake Bay model. Journal of Environmental Engineering. In press.
- Cercos, C. and T. Cole. 1993. Three dimensional eutrophication model of Chesapeake Bay. Journal of Environmental Engineering. 119:1006-1025
- Dennison, W., and R. Orth, K. Moore, J. Stevenson, V. Carter, S. Kollar, P. Bergstrom, and R. Batiuk. 1993. Assessing water quality with submersed aquatic vegetation. BioScience 43(2):86-94
- DiToro, D. and J. Fitzpatrick. 1993. Chesapeake Bay sediment flux model. Contract Report EL-93-2. US Army Engineer Waterways Experiment Station, Vicksburg MS.

- Evans, A., Webb, K., and Penhale, P. 1986. Photosynthetic acclimation in two coexisting seagrass systems, Zostera marina L. and Ruppia maritima L. Aquatic Botany, 24:185-197
- Gallegos, C., Correll, D., and Pierce, J. 1990. Modeling spectral diffuse attenuation, absorption, and scattering coefficients in a turbid estuary. Limnology and Oceanography, 35:1486-1502
- Gallegos, C. 1994. Refining habitat requirements of submersed aquatic vegetation: role of optical models. Estuaries, 17:187-199.
- Haller, W., and Sutton, D. 1975. Community structure and competition between hydrilla and vallisneria. Hyacinth Control Journal, 13:48-50.
- Holmes, R. 1970. The Secchi disk in turbid coastal water. Limnology and Oceanography 15:688-694
- Jassby, A., and Platt, T. 1976. Mathematical formulation of the relationship between photosynthesis and light for phytoplankton. Limnology and Oceanography 21:540-547.
- Johnson, B., Kim, K., Heath, R., Hsieh, B., and Butler, L. 1993. Validation of a three-dimensional hydrodynamic model of Chesapeake Bay. Journal of Hydraulic Engineering, 199(1):2-20.
- Keefe, C., Flemer, D., and Hamilton, D. 1976. Seston distribution in the Patuxent River estuary. Chesapeake Science 17(1):56-59
- Kemp, W., R. Twilley, J. Stevenson, W. Boynton, and J. Means. 1983. The decline of submerged vascular plants in the upper Chesapeake Bay: Summary of results concerning possible causes. Marine Technology Science Journal 17(2):78-89.
- Kirk, J. 1994. Light & Photosynthesis in Aquatic Ecosystems, 2<sup>nd</sup> edition, Cambridge University Press, Cambridge, 509 pp.
- Krause-Jensen, D., and Sand-Jensen, K. 1998. Light attenuation and photosynthesis of aquatic plant communities. Limnology and Oceanography, 43(3):396-407
- Linker, L., Stigall, C., Chang, C., and Donigian, A. (1996). Aquatic accounting: Chesapeake Bay watershed model quantifies nutrient loads, Water Environment and Technology, 8(1):48-52.
- Madden C. and W. Kemp. 1996. Ecosystem model of an estuarine submersed plant community: Calibration and simulation of eutrophication responses. Estuaries 19(2B):457-474.
- Marsh, J., Dennison, W., and Alberte, R. 1986. Effects of temperature on photosynthesis and respiration in eelgrass (Zostera marina L.). Journal of Experimental Marine Biology and Ecology 101:257-267
- Moore, K., Goodman, J., Stevenson, J., Murray, L., and Sundberg, K. 1994. Chesapeake Bay nutrients, light and SAV: Relations between variable water quality and SAV in field and mesocosm studies, Year 1 Draft Final Report, United States Environmental Protection Agency Chesapeake Bay Program, Annapolis MD.
- Moore, K., Wetzel, R., and Orth, R. 1997. Seasonal pulses in turbidity and their relations to eelgrass (Zostera

marina L.) survival in an estuary. Journal of Experimental Marine Biology and Ecology 215:115-134.

Moore, K., D. Wilcox, and R. Orth. 2000. Analysis of the abundance of submersed aquatic vegetation communities in the Chesapeake Bay. Estuaries. In press.

Neckles, H., Wetzel, R., and Orth, R. 1993. Relative effects of nutrient enrichment and grazing on epiphyte-macrophyte (zostera marina L.) dynamics. Oecologia 93:285-295.

Orth, R. and K. Moore. 1984. Distribution and abundance of submerged aquatic vegetation in Chesapeake Bay: An historical perspective. Estuaries 7(4B):531-540.

Penhale, P. 1977. Macrophyte - epiphyte biomass and productivity in an eelgrass (zostera marina L.) community. Journal of Experimental Marine Biology and Ecology 26:211-224.

Schubel, J. (1968). Turbidity maximum of the northern Chesapeake Bay, Science, 161, 1013-1015.

Staver, K. 1984. Responses of epiphytic algae to nitrogen and phosphorus enrichment and effects on productivity of the host plant, potamogeton perfoliatus L., in estuarine waters, Thesis submitted to the Faculty of the Graduate School of the University of Maryland in partial fulfillment of the requirements for the degree of Master of Science.

Thomann, R., Collier, J., Butt, A., Casman, E., and Linker, L. 1994. Technical analysis of response of Chesapeake Bay water quality model to loading scenarios. Technical Report Series 101/94, Chesapeake Bay Program Office, US Environmental Protection Agency, Annapolis, MD.

Titus, J., and Adams, M. 1979. Coexistence and comparative light relations of the submersed macrophytes Myrriophyllum spicatum L. and Vallisneria americana Michx. Oecologia (Berl.) 40:273-286.

Twilley, R., W. Kemp, K. Staver, J. Stevenson, and W. Boynton. 1985. Nutrient enrichment of estuarine submersed vascular plant communities. 1. Algal growth and effects on production of plants and associated communities. Marine Ecology Progress Series 23:179-191.

Van, T., Haller, W., and Bowes, G. 1976. Comparison of the photosynthetic characteristics of three submersed aquatic plants. Plant Physiology, 58:761-768

Ward, L., Kemp, W., and Boynton, W. 1984. The influence of waves and seagrass communities on suspended particulate matter in an estuarine embayment. Marine Geology, 59:85-103.

Wetzel, R., and Penhale, P. 1983. Production ecology of seagrass communities in the lower Chesapeake Bay. Marine Technology Society Journal, 17(2):22-32.

Wetzel, R., and H. Neckles. 1986. A model of Zostera marina L. photosynthesis and growth: Simulated effects of selected physical-chemical variables and biological interactions. Aquatic Botany 26:307-323

#### Sources of Unpublished Materials

Carter, V. United States Geological Survey, MS 430 National Center, Reston VA 22092

Lacouture, R. Smithsonian Environmental Research Center, Edgewater MD 21037

United States Environmental Protection Agency Chesapeake Bay Program, Annapolis MD 21403

Table 1. Parameters in SAV model					
Parameter	Definition	Freshwater	Ruppia	Zostera	Units
Acdw	carbon to dry weight ratio	0.37	0.37	0.37	
Acla	shoot carbon per unit leaf area	7.5	4.0	4.0	g shoot C m <sup>-2</sup> leaf area
Fpsr	fraction of production transferred from shoots to roots	0.12 to 1.0	0.1 to 0.85	0.1 to 0.85	
Ksh	light attenuation by shoots	0.045	0.045	0.045	m <sup>2</sup> g <sup>-1</sup> C
Kh <sub>nw</sub>	half-saturation concentration for nitrogen uptake by shoots	0.19	0.19	0.1	g N m <sup>-3</sup>
Kh <sub>ns</sub>	half-saturation concentration for nitrogen uptake by roots	0.95	0.95	0.4	g N m <sup>-3</sup>
Kh <sub>pw</sub>	half-saturation concentration for phosphorus uptake by shoots	0.028	0.028	0.02	g P m <sup>-3</sup>
Kh <sub>ps</sub>	half-saturation concentration for phosphorus uptake by roots	0.14	0.14	0.1	g P m <sup>-3</sup>
P <sub>max</sub>	maximum production at optimum temperature	0.1	0.08	0.06	g C g <sup>-1</sup> DW d <sup>-1</sup>
R <sub>sh</sub>	shoot respiration	0.022	0.022	0.015	d <sup>-1</sup>
R <sub>rt</sub>	root respiration	0.022	0.022	0.013	d <sup>-1</sup>
SL	sloughing	0.01 to 0.1	0.01 to 0.035	0.01 to 0.035	d <sup>-1</sup>
Trs	transfer from root to shoot	0.0 to 0.05	0.0	0.0	d <sup>-1</sup>
α	initial slope of PvsI curve	0.0075	0.002	0.0028	(g C g <sup>-1</sup> DW) (E m <sup>-2</sup> ) <sup>-1</sup>

Table 2. Parameters in epiphyte model			
Parameter	Definition	Value	Units
Acchl	carbon to chlorophyll ratio of viable epiphytes	75	$\text{g C g}^{-1} \text{Chl}$
Adwcep	ratio of epiphyte dry weight to viable epiphyte carbon	15	$\text{g DW g}^{-1} \text{C}$
Kep	light attenuation coefficient	0.1	$\text{m}^2 \text{ leaf surface g}^{-1} \text{ epiphyte C}$
Khep	density at which growth is halved	0.1	$\text{g epiphyte C g}^{-1} \text{ shoot C}$
Khn	half-saturation concentration for nitrogen uptake	0.025	$\text{g N m}^{-3}$
Khp	half-saturation concentration for phosphorus uptake	0.001	$\text{g P m}^{-3}$
Pep	maximum production at optimum temperature	300	$\text{g C g}^{-1} \text{Chl d}^{-1}$
PR	predation rate	1.0	$\text{g shoot C g}^{-1} \text{ epiphyte C d}^{-1}$
Rep	respiration	0.25	$\text{d}^{-1}$
$\alpha$	initial slope of PvsI curve	10	$(\text{g C g}^{-1} \text{Chl}) (\text{E m}^{-2})^{-1}$

This report is cited in the following way:  
Cercio, C.F. and K. Moore. 2001. System-Wide Submerged Aquatic  
Vegetation Model for the Chesapeake Bay January, 2001. Chesapeake  
Bay Program Office, Annapolis, MD.  
<http://www.chesapeakebay.net/modsc.htm> - *Publications Tab*. Date  
Retrieved: *retrieval date*